Human type I Fp	578	HWRKHTLSYVDVGTGKVTLEYRPVI DKTLNEADCATVPPAI RSY
Human type II Fp	578	HWRKHTLSFVDVGTGKVTLEYRPVI DKTLNEADCATIPPAI RSY
Rat Fp	570	HWRKHTLSYVDTKTGKVTLDYRPVI DKTLNEADCATVPPAI RSY
Mouse Fp	578	HWRKHTLSYVDI KTGKVTLEYRPVI DKTLNEADCATVPPAI RSY
Bovine Fp	582	HWRKHTLSYVDI KTGKVTLEYRPVI DRTLNETDCATVPPAI GSY
		Y586F V614I

Fig. 9. Alignment of amino acid sequences of Mammalian Fp subunits.Two amino acid residues in the red box are different in human Fp isoforms. Tyr 586 and Val 614 in type I Fp are changed to Phe 586 and Ile 614 in type II Fp, respectively. Tyr 586 and Val 614 are well conserved among mammals and no animals but humans have type II Fp [59].

all the examined tissues and many of the cultured cells showed abundant expression of type I Fp and optimum pH for this isoform is around physiological mitochondrial matrix pH (pH8.0).

Since type II Fp was expressed in some cancer cells, this isoform may play an important role in the metabolism of tumor tissue. To investigate the link between type II Fp and tumor tissue in detail, we analyzed mRNA expression ratio of Fp isoforms in several tissues including tumor tissues and cultured cells. Since some tumor marker genes are expressed in fetal tissues, we included the fetal tissues in this analysis.

As shown in Table 1, in cultured cells, all the normal cells tested showed mainly type I Fp expression as reported previously [59,60]. In tissues, expression of type I Fp was higher than that of type II Fp in all the organs tested including normal testes tissue. Interestingly, normal pancreatic tissue showed higher expression of type II Fp. In addition, several tumor tissues expressed predominantly type II Fp such as breast tumor, liver tumor, kidney tumor and cervix tumor. Among fetal tissues, brain and skeletal muscle showed higher expression of type II Fp than type I Fp.

4.4. Fumarate respiration of human cancer cells

Several observations suggested the presence of a reverse reaction of complex II, fumarate reductase (FRD), in mammalian cells, although no direct evidence of FRD activity in mammalian complex II has been available until recently [62,63]. The accumulation of succinate under hypoxic conditions has been reported, and complex II has been suggested to function as FRD in mammalian cells [64]. Metabolome analysis of the cancer cells supports this idea, because succinate, fumarate and malate were present at higher levels in cancer tissues than normal tissues [65]. FRD inhibitor pyrvinium pamoate, an anthelmintic, has also been reported to act as an anticancer compound in human cancer cells [62]. Furthermore, recent biochemical studies showed fumarate respiration in human mitochondria clearly [7,8]. Mitochondria isolated from DLD-1 cells showed FRD activity with 3 nmol/min/mg protein, although this number is quite lower than that of the *A. suum* mitochondria (200 nmol/min/mg). Interestingly, the cancer cells had higher FRD/SQR ratio than the normal cells. For example, FRD/SQR ratio in Panc-1 cells is 0.066 ± 0.010, while that in Human Dermal Fibroblast cells is 0.011 ± 0.002. In addition, FRD/SQR ratio increased when the cancer cells were cultured under hypoxic and glucose limited condition [7]. Effect of a treatment by phosphatase and protein kinase on the direction of enzyme activity of human complex II suggests the changes from SQR to QFR by phosphorylation of Fp.

Different from *A. suum*, which has at least two distinct complex IIs as mentioned previously, only one gene is found for each subunit of human complex II except Fp. In this connection, it is of interest to speculate that complex II with type II Fp has higher QFR activity and plays an important role in fumarate respiration in human mitochondria as terminal oxidase of the system. Further biochemical study on

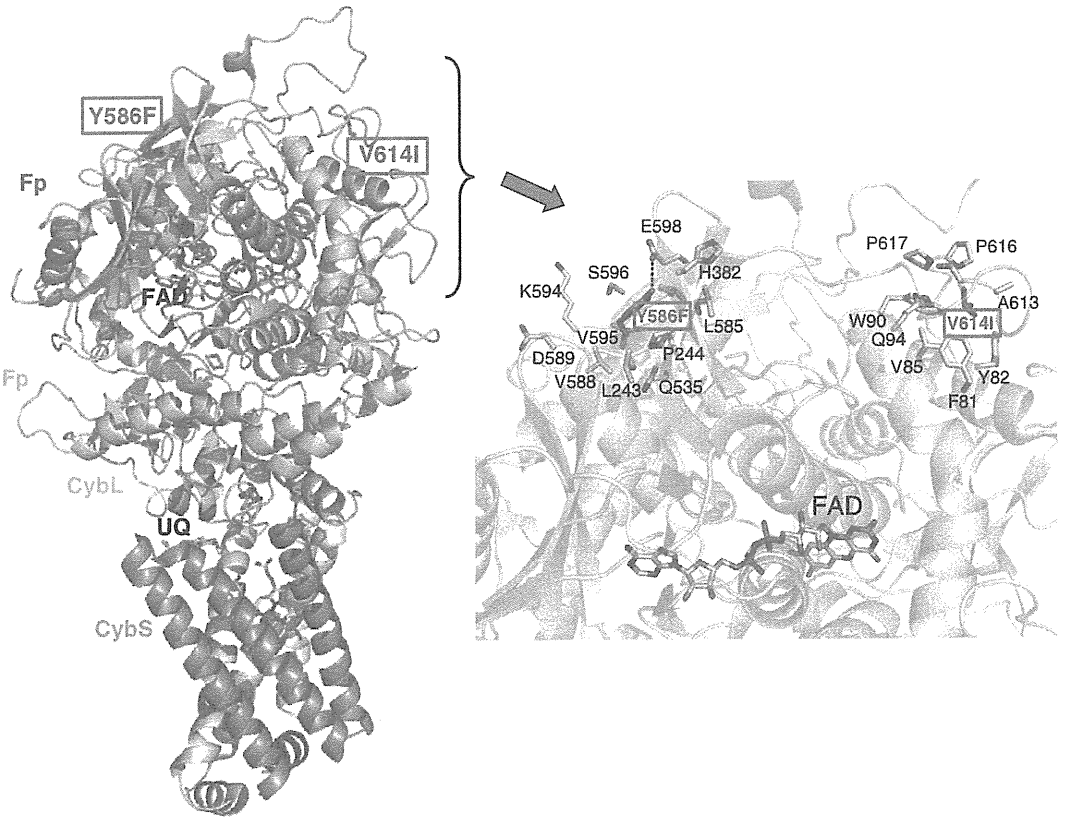

Fig. 10. Positions of Tyr 586 and Val 614 in the structure of porcine complex II.Two amino acid residues different in human isoforms, Y586F and V614I, shown in the cartoon representation of the porcine complex II structure (left) and the close-up view of the region including Y586F and V614I (right). V614I is surrounded mainly by hydrophobic residues, whereas Y586F by both hydrophilic and hydrophobic residues. Y586 and E598 are in the hydrogen bond distance (3.15 Å) to each other. UQ shows ubiquinone. The numbers of amino acid residues in the box represent the human amino acid sequences and the others are the porcine amino acid sequences.

Table 1
mRNA expression of Fp isoforms in human cultured cells and tissues.

The expression ratio of the two Fp isoforms was analyzed by RT-PCR-RFLP (restriction fragment length polymorphism with AvaII). Total RNAs were obtained from NIPPON GENE (Japan) for normal liver, heart, skeletal muscle, brain, kidney and breast tumor, colon tumor, stomach tumor and uterus tumor. Wako (Japan) for normal pancreas and fetal tissues. Invitrogen (USA) for normal testes and breast tumor, liver tumor, kidney tumor, colon tumor, pancreas tumor, cervix tumor, ovary tumor, prostate tumor. Cells; Fibroblast and Myoblast: kind gift from Dr. Yu-ichi Goto (National Institute of Neuroscience, Japan) A549, DLD-1 and MCF-7: kind gift from Mr. Yasuyuki Yamazaki (Taiho pharma ceutical, Japan) Panc-1: kind gift from Dr. Yasuhiro Esumi (National Cancer Institute, Japan) Raji: kind gift from Dr. Kazurou Shiomi (Kitasato university, Japan) HT-29, HU-VEC-C, MDA-M-231, BT-20 and T-47D: ATCC (USA). Pancreatic epithelial and stromal cells: DS pharma (Japan).

		Race	Gender	Age	I (%)/II (%)
Tissue (normal)	Liver*	Caucasoid	Female	15	70/30
	Heart*	Caucasoid	Pool of 7 donors		61/39
	Skeletal muscle*	--	Male	23	80/20
	Brain*	Caucasoid	Male	50	84/16
	Kidney*	Caucasoid	Pool of 8 donors		62/38
	Pancreas	--	Male	44	30/70
	Testes	Caucasoid	Male	19	100/0
Cell (normal)	Fibroblast*	Mongoloid	--	--	94/6
	Myoblast*	Mongoloid	--	--	87/13
	HUV-EC-C*	--	--	--	88/12
	Pancreatic epithelial	--	--	--	100/0
	Pancreatic stromal	--	--	--	100/0
Tissue (fetal)	Brain	--	Female	22 weeks	100/0
	Brain	--	Male	41 weeks	38/62
	Skeletal muscle	--	Male	22 weeks	0/100
	Skeletal muscle	--	Female	19 weeks	100/0
Tissue (cancer)	Breast	--	Female	55	100/0
	Breast	Mongoloid	Female	Pool of 6 donors	0/100
	Liver	Caucasoid	Male	60	0/100
	Kidney	Caucasioid	Female	54	23/77
	Colon	Caucasoid	Male	75	100/0
	Colon	--	--	--	100/0
	Pancreas	Mongoloid	Male	32	100/0
	Stomach	--	--	--	100/0
	Uterus	--	Female	--	100/0
	Cervix	Caucasoid	Female	59	23/77
	Ovary	Caucasoid	Female	32	100/0
	Prostate	--	Male	--	100/0
Cell (cancer)	HT29*	Caucasoid	Female	44	92/8
	A549*	Caucasoid	Male	58	96/4
	DLD-1*	--	Male	--	25/75
	MCF-7*	Caucasoid	Female	69	23/77
	Raji*	Neglod	Male	11	17/83
	Panc-1	Caucasoid	Male	56	12/88
	MDA-M-231	Caucasoid	Female	51	100/0
	BT-20	Caucasoid	Female	78	78/22
	T-47D	Caucasoid	Female	54	53/47

* Tomitsuka, et al. [59,60].

the difference between type I and type II Fp will bring final conclusion on this attractive idea.

5. Conclusions

The recent findings described in this review indicate that the respiratory chain plays an important role in responses to changes in the amount of oxygen in the environment. Complex II functions as a fumarate reductase during adaptation to a hypoxic condition to ensure the maintenance of oxygen homeostasis. In this connection, the reports indicating that complex II functions as an oxygen sensor are of great interest [63].

In addition, direct evidence of fumarate respiration in human mitochondria are quite important in the study of energy metabolism in hypoxic condition including cancer cells. Differences in energy metabolism between hosts and parasites and/or cancer cells are attractive therapeutic targets.

Acknowledgements

This work was supported in part by Creative Scientific Research Grant 18GS0314 (to KK), Grant-in-aid for Scientific Research on Priority Areas 18073004 (to KK) from the Japanese Society for the Promotion of Science, and Targeted Proteins Research Program (to KK) from the Japanese Ministry of Education, Science, Culture, Sports and Technology (MEXT).

References

[1] K. Kita, K. Shiomi, S. Ōmura, Parasitology in Japan: advances in drug discovery and biochemical studies, Trends Parasitol. 23 (2007) 223–229.
[2] A. Kroger, V. Geisler, E. Lemma, F. Theis, R. Lenger, Bacterial fumarate respiration, Arch. Microbiol. 158 (1992) 311–314.
[3] T. Kuramochi, H. Hirawake, S. Kojima, S. Takamiya, R. Furushima, T. Aoki, R. Komuniecki, K. Kita, Sequence comparison between the flavoprotein subunit of the fumarate reductase (complex II) of the anaerobic parasitic nematode, *Ascaris suum* and the succinate dehydrogenase of theaerobic, free-living nematode, *Caenorhabditis elegans*, Mol. Biochem. Parasitol. 68 (1994) 177–187.
[4] F. Saruta, H. Hirawake, S. Takamiya, Y.-C. Ma, T. Aoki, K. Sekimizu, S. Kojima, K. Kita, Cloning of a cDNA encoding the small subunit of cytochrome b_{558} (cybS) of mitochondrial fumarate reductase (complex II) from adult *Ascaris suum*, Biochim. Biophys. Acta 1276 (1996) 1–5.
[5] H. Amino, H. Wang, H. Hirawake, F. Saruta, D. Mizuchi, R. Mineki, N. Shindo, K. Murayama, S. Takamiya, T. Aoki, S. Kojima, K. Kita, Stage-specific isoforms of *Ascaris suum* complex II: the fumarate reductase of the parasitic adult and the succinate dehydrogenase of free-living larvae share a common iron-sulfur subunit, Mol. Biochem. Parasitol. 106 (2000) 63–76.
[6] K. Kita, S. Takamiya, Electron-transfer complexes in *Ascaris* mitochondria, Adv. Parasitol. 51 (2002) 95–131.
[7] E. Tomitsuka, K. Kita, H. Esumi, Regulation of succinate–ubiquinone reductase and fumarate reductase activities in human complex II by phosphorylation of its flavoprotein subunit, Proc. Jpn. Acad. Ser. B Phys. Biol. Sci. 85 (2009) 258–265.
[8] E. Tomitsuka, K. Kita, H. Esumi, The NADH-fumarate reductase system, a novel mitochondrial energy metabolism, is a new target for anticancer therapy in tumor microenvironments, Ann. N. Y. Acad. Sci. 201 (2011) 44–49.
[9] M.P. Paranagama, K. Sakamoto, H. Amino, M. Awano, H. Miyoshi, K. Kita, Contribution of the FAD and quinone binding sites to the production of reactive oxygen species from *Ascaris suum* mitochondrial complex II, Mitochondrion 10 (2010) 158–165.
[10] R.D. Guzy, B. Sharma, E. Bell, N.S. Chandel, P.T. Schumacker, Loss of the SdhB, but Not the SdhA, subunit of complex II triggers reactive oxygen species-dependent hypoxia-inducible factor activation and tumorigenesis, Mol. Cell. Biol. 28 (2008) 718–731.
[11] M.A. Selak, S.M. MacKenzie, H. Boulahbel, D.G. Watson, K.D. Mansfield, Y. Pan, M.C. Simon, C.B. Thompson, E. Gottlieb, Succinate links TCA cycle dysfunction to oncogenesis by inhibiting HIF-alpha prolyl hydroxylase, Cancer Cell 7 (2005) 77–85.
[12] R. Komuniecki, B.G. Harris, J. Marr, M. Mueller, Biochemistry and Molecular Biology of Parasites, Academic Press, London, 1995, pp. 49–66.
[13] A.G.M. Tielens, J. Van Hellemond, The electron transport chain in anaerobically functioning eukaryotes, Biochim. Biophys. Acta 1365 (1998) 71–78.
[14] K. Kita, H. Hirawake, S. Takamiya, Cytochromes in the respiratory chain of helminth mitochondria, Int. J. Parasitol. 27 (1997) 617–630.
[15] J. Matsumoto, K. Sakamoto, N. Shinjyo, Y. Kido, N. Yamamoto, K. Yagi, H. Miyoshi, N. Nonaka, K. Katakura, K. Kita, Y. Oku, Anaerobic NADH-fumarate reductase system is predominant in the respiratory chain of *Echinococcus multilocularis*, providing a novel target for the chemotherapy of alveolar echinococcosis, Antimicrob. Agents Chemother. 52 (2008) 164–170.
[16] P. Kohler, R. Bachmann, Mechanisms of respiration and phosphorylation in *Ascaris* muscle mitochondria, Mol. Biochem. Parasitol. 1 (1980) 75–90.
[17] H. Oya, K. Kita, in: E. Bennet, C. Behm, C. Bryant (Eds.), Comparative Biochemistry of Parasitic Helminths, Chapman and Hall, London, 1988, pp. 35–53.
[18] S. Takamiya, R. Furushima, R.H. Oya, Electron transfer complexes of *Ascaris suum* muscle mitochondria: I. Characterization of NADH-cytochrome *c* reductase (complex I–III), with special reference to cytochrome localization, Mol. Biochem. Parasitol. 13 (1984) 121–134.
[19] S. Takamiya, K. Kita, H. Wang, P.P. Weinstein, A. Hiraishi, H. Oya, T. Aoki Developmental, Changes in the respiratory chain of *Ascaris* mitochondria, Biochim. Biophys. Acta 1141 (1993) 65–74.
[20] S.T. Cole, C. Condon, B.D. Lemire, J.H. Weiner, Molecular biology, biochemistry and bioenergetics of fumarate reductase, a complex membrane-bound iron–sulfur flavoenzyme of *Escherichia coli*, Biochim. Biophys. Acta 811 (1985) 381–403.
[21] A. Hiraishi, Fumarate reduction systems in members of the family *Rhodospirillaceae* with different quinone types, Arch. Microbiol. 150 (1988) 56–60.
[22] F. Iwata, N. Shinjyo, H. Amino, K. Sakamoto, M.K. Islam, N. Tsuji, K. Kita, Change of subunit composition of mitochondrial complex II (succinate–ubiquinone reductase/quinol–fumarate reductase) in *Ascaris suum* during the migration in the experimental host, Parasitol. Int. 57 (2008) 54–61.

[23] T.M. Iverson, C. Luna-Chavez, G. Cecchini, D.C. Rees, Structure of the *Escherichia coli* fumarate reductase respiratory complex, Science 284 (1999) 1961–1966.
[24] C.R. Lancaster, A. Kröger, M. Auer, H. Michel, Structure of fumarate reductase from *Wolinella succinogenes* at 2.2 A resolution, Nature 402 (1999) 377–385.
[25] K. Kita, C. Vibat, S. Meinhardt, J. Guest, R. Gennis, One-step purification from *Escherichia coli* of complex II (succinate: ubiquinone oxidoreductase) associated with succinate-reducible cytochrome b_{556}, J. Biol. Chem. 264 (1989) 2672–2677.
[26] G. Cecchini, I. Schroder, R.P. Gunsalus, E. Maklashina, Succinate dehydrogenase and fumarate reductase from *Escherichia coli*, Biochim. Biophys. Acta 1553 (2002) 140–157.
[27] C.R.D. Lancaster, Structure and function of succinate: quinone oxidoreductases and the role of quinol: fumarate reductases in fumarate respiration, in: D. Zannoni (Ed.), Respiration in Archaea and Bacteria: Diversity of Prokaryotic Electron Transport Carriers, Kluwer Academic Publishers, The Netherlands, 2004, pp. 57–85.
[28] J.J. Van Hellmond, A. van der Klei, S.W.H. van Weelden, A.G.M. Tielens, Biochemical and evolutionary aspects of anaerobically functioning bacteria, Philos. Trans. R. Soc. B 358 (2003) 205–215.
[29] K. Kita, H. Hirawake, H. Miyadera, H. Amino, S. Takeo, Role of complex II in anaerobic respiration of the parasite mitochondria from *Ascaris suum* and *Plasmodium falciparum*, Biochim. Biophys. Acta 1553 (2002) 123–139.
[30] H.P. Indo, M. Davidson, H.C. Yen, S. Suenaga, K. Tomita, T. Nishii, M. Higuchi, Y. Koga, T. Ozawa, H.J. Majima, Evidence of ROS generation by mitochondria in cells with impaired electron transport chain and mitochondrial DNA damage, Mitochondrion 7 (2007) 106–118.
[31] P. Jezek, L. Hlavata, Mitochondria in homeostasis of reactive oxygen species in cell, tissues, and organism, Int. J. Biochem. Cell Biol. 37 (2005) 2478–2503.
[32] M.P. Murphy, How mitochondria produce reactive oxygen species, Biochem. J. 417 (2009) 1–13.
[33] J. St-Pierre, J.A. Buckingham, S.J. Roebuck, M.D. Brand, Topology of superoxide production from different sites in the mitochondrial electron transport chain, J. Biol. Chem. 277 (2002) 44784–44790.
[34] I.K. Srivastava, H. Rottenberg, A.B. Vaidya, Atovaquone, a broad spectrum antiparasitic drug, collapses mitochondrial membrane potential in a malarial parasite, J. Biol. Chem. 272 (1997) 3961–3966.
[35] S. Looareesuwan, C. Viravan, H.K. Webster, D.E. Kyle, D.B. Hutchinson, C.J. Canꝺ eld, Clinical studies of atovaquone, alone or in combination with other antimalarial drugs, for treatment of acute uncomplicated malaria in Thailand, Am. J. Trop. Med. Hyg. 54 (1996) 62–66.
[36] D. Syafruddin, J.E. Siregar, S. Marzuki, Mutations in the cytochrome *b* gene of *Plasmodium berghei* conferring resistance to atovaquone, Mol. Biochem. Parasitol. 104 (1999) 185–194.
[37] I.K. Srivastava, J.M. Morrisey, E. Darrouzet, F. Daldal, A.B. Vaidya, Resistance mutations reveal the atovaquone-binding domain of cytochrome *b* in malaria parasites, Mol. Microbiol. 33 (1999) 704–711.
[38] P. Kohler, R. Bachmann, The effects of the antiparasitic drugs levamisole, thiabendazole, praziquantel, and chloroquine on mitochondrial electron transport in muscle tissue from *Ascaris suum*, Mol. Biochem. Parasitol. 14 (1978) 155–163.
[39] A. Armson, W.B. Grubb, A.H.W. Mendis, The effect of electron transport (ET) inhibitors and thiabendazole on the fumarate reductase (FR) and succinate dehydrogenase (SDH) of *Strongyloides ratti* infective (L3) larvae, Int. J. Parasitol. 25 (1995) 261–263.
[40] S. Omura, H. Miyadera, H. Ui, K. Shiomi, Y. Yamaguchi, R. Masuma, T. Nagamitsu, D. Takano, T. Sunazuka, A. Harder, H. Kölbl, M. Namikoshi, H. Miyoshi, K. Sakamoto, K. Kita, An anthelmintic compound, nafuredin, shows selective inhibition of complex I in helminth mitochondria, Proc. Natl. Acad. Sci. U. S. A. 98 (2001) 60–62.
[41] T. Yamashita, T. Ino, H. Miyoshi, K. Sakamoto, A. Osanai, E. Nakamaru-Ogiso, K. Kita, Rhodoquinone reaction site of mitochondrial complex I, in parasitic helminth, *Ascaris suum*, Biochim. Biophys. Acta 1608 (2004) 97–103.
[42] H. Miyadera, K. Shiomi, H. Ui, Y. Yamaguchi, R. Masuma, H. Tomoda, H. Miyoshi, A. Osanai, K. Kita, S. Omura, Atpenins, potent and specific inhibitors of mitochondrial complex II (succinate-ubiquinone oxidoreductase), Proc. Natl. Acad. Sci. U. S. A. 100 (2003) 473–477.
[43] A. Osanai, S. Harada, K. Sakamoto, H. Shimizu, D.K. Inaoka, K. Kita, Crystallization of mitochondrial rhodoquinol–fumarate reductase from the parasitic nematode *Ascaris suum* with the specific inhibitor flutolanil, Acta Crystallogr. Sect. F Struct. Biol. Cryst. Commun. 65 (2009) 941–954.
[44] V. Yankovskaya, R. Horsefield, S. Törnroth, C. Luna-Chavez, H. Miyoshi, C. Léger, B. Byrne, G. Cecchini, S. Iwata, Architecture of succinate dehydrogenase and reactive oxygen species generation, Science 299 (2003) 700–704.
[45] F. Sun, X. Huo, Y. Zhai, A. Wang, J. Xu, D. Su, M. Bartlam, Z. Rao, Crystal structure of mitochondrial respiratory membrane protein complex II, Cell 121 (2005) 1043–1057.
[46] L.S. Huang, G. Sun, D. Cobessi, A.C. Wang, J.T. Shen, E.Y. Tung, V.E. Anderson, E.A. Berry, 3-nitropropionic acid is a suicide inhibitor of mitochondrial respiration that, upon oxidation by complex II, forms a covalent adduct with a catalytic base arginine in the active site of the enzyme, J. Biol. Chem. 281 (2006) 5965–5972.
[47] J.P. Bayley, P. Devilee, E.M.P. Taschner, The SDH mutation database: an online resource for succinate dehydrogenase sequence variants involved in pheochromocytoma, paraganglioma and mitochondrial complex II deficiency, BMC Med. Genet. 6 (2005) 39.
[48] B.E. Baysal, On the association of succinate dehydrogenase mutations with hereditary paraganglioma, Trends Endocrinol. Metab. 14 (2003) 453–459.
[49] C. Eng, M. Kiuru, M.J. Fernandez, L.A. Aaltonen, A role for hypoxic mitochondrial enzymes in inherited neoplasia and beyond, Nat. Rev. Cancer 3 (2003) 193–202.
[50] P.J. Pollard, N.C. Wortham, I.P. Tomlinson, The TCA cycle and tumorigenesis: the examples of fumarate hydratase and succinate dehydrogenase, Ann. Med. 35 (2003) 632–639.
[51] P. Rustin, A. Rotig, Inborn errors of complex II–unusual human mitochondrial diseases, Biochim. Biophys. Acta 1553 (2002) 117–122.
[52] N. Ishii, T. Ishii, P.S. Hartman, The role of the electron transport SDHC gene on lifespan and cancer, Mitochondrion 7 (2007) 24–38.
[53] H.X. Hao, O. Khalimonchuk, M. Schraders, N. Dephoure, J.P. Bayley, H. Kunst, P. Devilee, C.W. Cremers, J.D. Schiffman, B.G. Bentz, S.P. Gygi, D.R. Winge, H. Kremer, J. Rutter, SDH5, a gene required for flavination of succinate dehydrogenase, is mutated in paraganglioma, Science 325 (2009) 1139–1142.
[54] M.A. Birch-Machin, R.W. Taylor, B. Cochran, B.A. Ackrell, D.M. Turnbull, Late-onset optic atrophy, ataxia, and myopathy associated with a mutation of a complex II gene, Ann. Neurol. 48 (2000) 330–335.
[55] T. Bourgeron, P. Rustin, D. Chretien, M. Birch-Machin, M. Bourgeois, E. Viegas-Pequignot, A. Munnich, A. Rotig, Mutation of a nuclear succinate dehydrogenase gene results in mitochondrial respiratory chain deficiency, Nat. Genet. 11 (1995) 144–149.
[56] B. Parfait, D. Chretien, A. Rötig, C. Marsac, A. Munnich, P. Rustin, Compound heterozygous mutations in the flavoprotein gene of the respiratory chain complex II in a patient with Leigh syndrome, Hum. Genet. 106 (2000) 236–243.
[57] R. Van Coster, S. Seneca, J. Smet, R. Van Hecke, E. Gerlo, B. Devreese, J. Van Beeumen, J.G. Leroy, L. De Meirleir, W. Lissens, Homozygous Gly555Glu mutation in the nuclear-encoded 70 kDa flavoprotein gene causes instability of the respiratory chain complex II, Am. J. Med. Genet. A 120 (2003) 13–18.
[58] D. Ghezzi, P. Goffrini, G. Uziel, R. Horvath, T. Klopstock, H. Lochmüller, P. D'Adamo, P. Gasparini, T.M. Strom, H. Prokisch, F. Invernizzi, I. Ferrero, M. Zeviani, SDHAF1, encoding a LYR complex-II specific assembly factor, is mutated in SDH-defective infantile leukoencephalopathy, Nat. Genet. 41 (2009) 654–656.
[59] E. Tomitsuka, H. Hirawake, Y. Goto, M. Taniwaki, S. Harada, K. Kita, Direct evidence for two distinct forms of the flavoprotein subunit of human mitochondrial complex II (succinate–ubiquinone reductase), J. Biochem. 134 (2003) 191–195.
[60] E. Tomitsuka, Y. Goto, M. Taniwaki, K. Kita, Direct evidence for expression of type II flavoprotein subunit in human complex II (succinate–ubiquinone reductase), Biochem. Biophys. Res. Commun. 311 (2003) 74–79.
[61] M. Salvi, N. Morrice, A. Brunati, A. Toninello, Identification of the flavoprotein of succinate dehydrogenase and aconitase as in vitro mitochondrial substrates of Fgr tyrosine kinase, FEBS Lett. 581 (2007) 5579–5585.
[62] H. Esumi, J. Lu, Y. Kurashima, T. Hanaoka, Antitumor activity of pyrvinium pamoate, 6-(dimethylamino)-2-[2-(2,5-dimethyl-1-phenyl-1H-pyrrol-3-yl)ethenyl]-1-me thyl-quinolinium pamoate salt, showing preferential cytotoxicity during glucose starvation, Cancer Sci. 95 (2004) 685–690.
[63] B.E. Baysal, R.E. Ferrell, J.E. Willett-Brozick, E.C. Lawrence, D. Myssiorek, A. Bosch, A. van der Mey, P.E. Taschner, W.S. Rubinstein, E.N. Myers, C.W. Richard, C.J. Cornelisse, P. Devilee, B. Devlin, Mutations in SDHD, a mitochondrial complex II gene, in hereditary paraganglioma, Science 287 (2000) 848–851.
[64] J.M. Weinberg, M.A. Venkatachalam, N.F. Roeser, I. Nissim, Mitochondrial dysfunction during hypoxia/reoxygenation and its correction by anaerobic metabolism of citric acid cycle intermediates, Proc. Natl. Acad. Sci. U. S. A. 97 (2000) 2826–2831.
[65] A. Hirayama, K. Kami, M. Sugimoto, M. Sugawara, N. Toki, H. Onozuka, T. Kinoshita, N. Saito, A. Ochiai, M. Tomita, H. Esumi, T. Soga, Quantitative metabolome profiling of colon and stomach cancer microenvironment by capillary electrophoresis time-of-flight mass spectrometry, Cancer Res. 69 (2009) 4918–4925.

J. Biochem. 2012;151(6):589–592 doi:10.1093/jb/mvs051

JB THE JOURNAL OF BIOCHEMISTRY

Rapid communication

Crystal structure of mitochondrial quinol–fumarate reductase from the parasitic nematode *Ascaris suum*

Received April 18, 2012; accepted May 1, 2012; published online May 9, 2012

Hironari Shimizu[1], Arihiro Osanai[1], Kimitoshi Sakamoto[1], Daniel Ken Inaoka[1], Tomoo Shiba[2], Shigeharu Harada[2,*] and Kiyoshi Kita[1,†]

[1]Department of Biomedical Chemistry, Graduate School of Medicine, University of Tokyo, 7-3-1 Hongo, Bunkyo-ku, Tokyo 113-0033; and [2]Department of Applied Biology, Graduate School of Science and Technology, Kyoto Institute of Technology, Sakyo-Ku, Kyoto 606-8585, Japan

*Shigeharu Harada, Department of Applied Biology, Graduate School of Science and Technology, Kyoto Institute of Technology, Sakyo-ku, Kyoto 606-8585, Japan. Tel: +81-75-724-7541; Fax: +81-75-724-7541, email: harada@kit.ac.jp

†Kiyoshi Kita, Department of Biomedical Chemistry, Graduate School of Medicine, University of Tokyo, 7-3-1 Hongo, Bunkyo-ku, Tokyo 113-0033, Japan. Tel: +81-3-5841-3526, Fax: +81-3-5841-3444, email: kitak@m.u-tokyo.ac.jp

In the anaerobic respiratory chain of the parasitic nematode *Ascaris suum*, complex II couples the reduction of fumarate to the oxidation of rhodoquinol, a reverse reaction catalyzed by mammalian complex II. In this study, the first structure of anaerobic complex II of mitochondria was determined. The structure, composed of four subunits and five co-factors, is similar to that of aerobic complex II, except for an extra peptide found in the smallest anchor subunit of the *A. suum* enzyme. We discuss herein the structure–function relationship of the enzyme and the critical role of the low redox potential of rhodoquinol in the fumarate reduction of *A. suum* complex II.

Keywords: *Ascaris suum*/crystal structure/mitochondrial respiratory complex II/rhodoquinol–fumarate reductase (QFR)/reaction mechanism.

Abbreviations: $C_{10}M$, *n*-decyl-β-D-maltoside; $C_{12}M$, *n*-dodecyl-β-D-maltoside; C_nE_m, *n*-alkyl ethylene glycol monoether; CybL, cytochrome *b* large subunit of complex II; CybS, cytochrome *b* small subunit of complex II; FAD, flavin adenine dinucleotide; Fp, flavoprotein subunit; Ip, iron–sulphur subunit; NADH, nicotinamide adenine dinucleotide; PEG, polyethyleneglycol; QFR, quinol–fumarate reductase; RQ, rhodoquinone; RQH_2, rhodoquinol; SML, sucrose monolaurate; SQR, succinate–ubiquinone reductase.

The anaerobic respiratory chain, known as the NADH-fumarate reductase (NADH-FRD) system, plays an essential role in the anaerobic energy metabolism of adult *Ascaris suum*, a parasite that inhabits the small intestine, an environment with low oxygen tension (pO_2 of ~4 mmHg). The NADH-FRD system comprises two membrane proteins, complexes I and II, embedded in the mitochondrial inner membrane. Complex I (NADH–rhodoquinone reductase) reduces rhodoquinone (RQ) to rhodoquinol (RQH_2) using the reducing equivalent of NADH, and complex II, which functions as a RQH_2–fumarate reductase (QFR), couples the reduction of fumarate to succinate to the oxidation of RQH_2 to RQ, a reverse reaction catalysed by mammalian complex II (succinate–ubiquinone reductase, SQR) of the aerobic respiratory chain. The anaerobic NADH-fumarate reductase system is found not only in *A. suum* but also in bacteria and many other parasites, and is thus a promising target for chemotherapy (*1-3*).

Although no structure is currently available for eukaryotic QFR-type complex II, structures of SQR-type complex II from porcine (*4*), avian (*5*) and *Escherichia coli* (*6*), as well as those of QFR-type from *E. coli* (*7*) and *Wolinella succinogenes* (*8*), have been determined. Their structures are similar to each other and are generally composed of four polypeptides, the largest flavoprotein subunit (Fp, 70 kDa), an iron–sulphur cluster subunit (Ip, 30 kDa), and cytochrome *b* large (CybL, 15 kDa), and small (CybS, 13 kDa) subunits. In this study, the first X-ray structural analysis of a eukaryotic QFR-type complex II was performed for *A. suum* adult complex II (*A. suum* QFR) in order to clarify the factors responsible for its QFR activity and the mechanisms of RQH_2 oxidation coupled to fumarate reduction.

Ascaris suum QFR was extracted and purified from adult *A. suum* muscle mitochondria and crystallized according to the method described by Osanai *et al.* (*9*). In brief, ~4 kg of *A. suum* obtained from a local slaughterhouse was minced and suspended in Chappell-Perry medium (100 mM KCl, 50 mM Tris–HCl pH 7.4, 5 mM magnesium sulphate, 1 mM ATP, 1 mM EDTA). The fraction containing mitochondria was separated by differential centrifugation, and *A. suum* QFR was then solubilized using 1.0% (w/v) sucrose monolaurate (SML; Dojindo). After purification with anion-exchange column chromatography, SML was exchanged with a mixture of octaethylene glycol monododecyl ether ($C_{12}E_8$) and dodecyl maltoside ($C_{12}M$) by repeated PEG3350 precipitation and dissolution in a buffer containing 0.6% (w/v) $C_{12}E_8$, 0.4% (w/v) $C_{12}M$, 200 mM NaCl, 10 mM Tris–HCl pH 7.5 and 1 mM sodium malonate. Crystallization was performed by the dialysis method using a reservoir solution containing 15% (w/v) PEG3350, 100 mM Tris–HCl pH 8.4, 200 mM NaCl,

1 mM sodium malonate, 0.06% (w/v) $C_{12}E_8$ and 0.04% (w/v) $C_{12}M$. Reddish crystals grew to 100–200 μm in 2–3 days. Crystals of *A. suum* QFR in complex with fumarate were prepared by soaking crystals in the reservoir solution supplemented with 1 mM of sodium fumarate instead of sodium malonate.

X-ray diffraction experiments were performed under a N_2 gas stream (100 K) at SPring-8 beam line BL44XU (Bruker DIP-6040 detector) and at Photon Factory beam line NW12 (ADSC315 CCD detector). Data were processed and scaled using *HKL2000* (*10*). The initial structural model of *A. suum* QFR was solved by molecular replacement using the structure of porcine complex II (pdb code: 1ZOY) as a search model. *Molrep* (*11*) was used for molecular replacement. The refinement of the structure and model building were performed using *Refmac5* (*12*) and *Coot* (*13*), respectively. Data processing and refinement statistics are shown in Supplementary Table SI. All figures were generated using *PyMOL* (*14*). The coordinates have been deposited in the Protein Data Bank under ID codes 3VR8 and 3VRB for the malonate and fumarate bound forms, respectively.

The X-ray structure of *A. suum* QFR (Fig. 1A and B) is composed of Fp, Ip, CybL and CybS subunits, with two molecules in the asymmetric unit (chains A–D and E–H, respectively). As there are no significant differences between the overall protein structures of 3VR8 and 3VRB, we will focus on chains A–D of the malonate-bound form to describe the protein structure as a whole. Fp (chain A) and Ip (chain B) are hydrophilic, whereas CybL (chain C) and CybS (chain D) are hydrophobic membrane-integrated subunits. Fp comprises four domains: a FAD binding domain (residues A33–A279 and A384–A465), a capping domain (A279–A384), a helical domain (A465–A580) and a C-terminal domain (A580–A645). A FAD prosthetic group is held in the FAD binding domain by a covalent bond to His A79 and by hydrogen bonds with highly conserved residues (Ala A49, Thr A71, Lys A72, Met A73, Ser A78, Thr A80, Gln A84, Gly A85, Gly A86, Ala A201, Asp A255, Glu A421, Arg A432, Ser A437, Leu A438) across amino acid sequences of complex IIs from various species. Ip contains an N-terminal plant ferredoxin-like domain (residues B33–B130) and a C-terminal bacterial ferredoxin-like domain (B130–B281). Of the three iron–sulphur centres bound to Ip, [2Fe–2S] is coordinated by four cysteine residues (B89, B94, B97 and B109) and located in the N-terminal domain, whereas [4Fe–4S] and [3Fe–4S] that are coordinated by four (B182, B185, B188 and B249) and three (B192, B239 and B245) cysteine residues, respectively, are bound to the C-terminal domain. These iron–sulphur centres are also surrounded with highly conserved hydrophobic amino acid residues (Fig. 1C). The structures of Fp and Ip are similar to those of complex IIs with known structures, such as *E. coli* SQR (*6*), *E. coli* QFR (*7*), *W. succinogens* QFR (*8*), porcine SQR (*4*) and avian SQR (*5*).

In contrast to Fp and Ip, the hydrophobic membrane-spanning part shows diversity among species. In *W. succinogens* QFR, it consists of a single polypeptide chain and two haem *b* prosthetic groups, whereas *A. suum* QFR, like *E. coli* SQR, porcine SQR and avian SQR, holds two polypeptide chains (CybL and CybS) and one haem *b*. Both CybL and CybS consist of three membrane-spanning α-helices

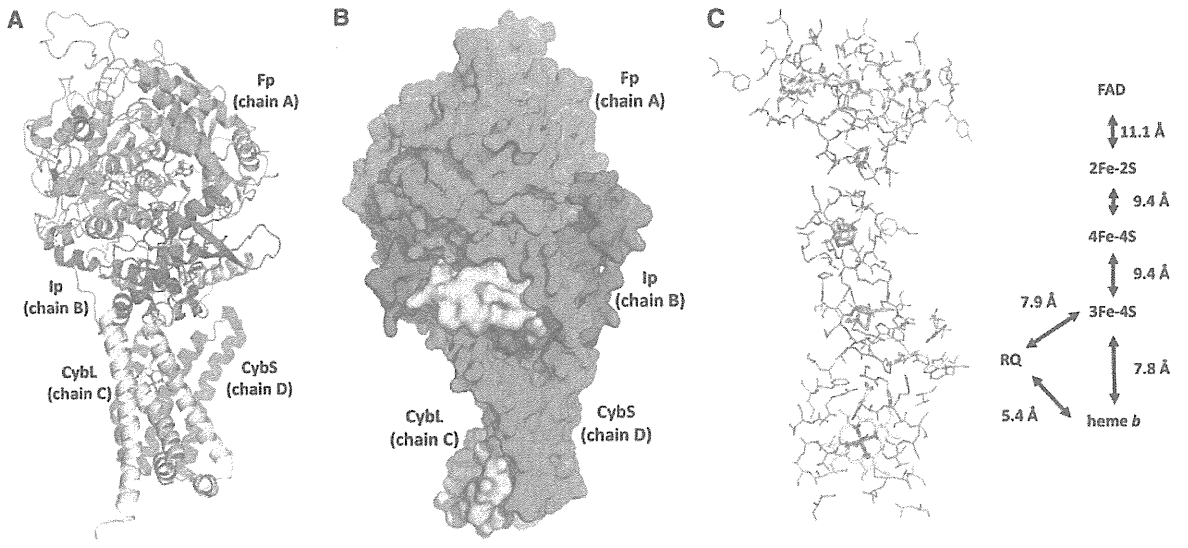

Fig. 1 Structure of *A. suum* QFR. Fp (chain A), Ip (chain B), CybL (chain C) and CybS (chain D) are coloured in green, red, yellow and cyan, respectively. Colour code for each atom type: C (yellow), N (blue), O (red), S (orange) and Fe (brown). (A) Cartoon representation of the *A. suum* QFR structure. FAD, iron–sulphur centres and haem *b* are shown as sticks. (B) Surface model of *A. suum* QFR viewed from a different direction from (A) for easy observation of the extra polypeptide attached to the N-terminus of CybS. (C) The arrangement of FAD, [2Fe–2S], [4Fe–4S], [3Fe–4S], haem *b* and RQ. Their edge-to-edge distances are also shown. Amino acid residues within 5 Å of the prosthetic groups and RQ are shown by a wire model. Conserved residues across amino acid sequences of complex IIs are coloured in magenta.

(Fig. 1A and B) and anchor the *A. suum* QFR to the membrane. A haem *b* is embedded into the interface between the CybL and CybS, and two conserved His residues (His C131 and His D95) are ligated to the haem iron. A distinct cleft, whose location is in agreement with the quinone binding sites proposed for other complex IIs, is formed by Ip, CybL and CybS, and a residual electron density probably revealing a bound RQ is detected in the cleft.

Figure 1C shows the arrangement of the prosthetic groups bound to *A. suum* QFR and their edge-to-edge distances. [2Fe–2S], [4Fe–4S] and [3Fe–4S] line between FAD and RQ as observed in other complex IIs (*15*). Thus, the disposition of the prosthetic groups is critical to allow electron transfer from RQH_2 to FAD via the iron–sulphur centres. The hydrophobic environment around the iron–sulphur centres and distances between neighbouring centres (<14 Å) suggest that the electron transfer from RQH_2 to FAD is carried out by quantum tunneling (*16*), as proposed for *E. coli* SQR (*6*).

Figure 2A shows that fumarate is bound near the FAD isoalloxazine ring in a non-planar conformation. C2, C3 and C4 carboxyl group are in the same plane parallel to the isoalloxazine ring, whereas the C1 carboxyl group is twisted around the C1 and C2 bond with a C3–C2–C1–O1A dihedral angle of 83.7°. The twisting, which is stabilized by hydrogen bonds with Gly A85, Thr A288, Glu A289 and Arg A320, suggests that the uniform distribution of π-electrons over the conjugated double bonds of fumarate is broken and a partial charge separation, $C2^{\delta+}$ and $C3^{\delta-}$, is induced. The contact of $C2^{\delta+}$ with FAD N5 (4.05 Å) suggests that a hydride (or hydride equivalent) is transferred from reduced FAD N5 to $C2^{\delta+}$ in the reduction of fumarate with the reduced FAD. Arg A320 is a probable candidate that supplies a proton to $C3^{\delta-}$ to complete the reduction of fumarate. The twisted conformation of fumarate is also observed in flavoproteins with fumarate reductase acitivity (1D4E, 1P2E, 1QLB and 2E6D), and a similar mechanism is proposed for *E. coli* QFR (*17*) and *Trypanosoma cruzi* dihydroorotate dehydrogenase (*18*).

Figure 2B shows the structure of the RQ binding site proposed for *A. suum* QFR. The site is formed by Ip, CybL and CybS, and is in agreement with ubiquinone binding sites suggested for other complex IIs. [3Fe–4S] is the nearest iron–sulphur centre to RQ (9.2 and 7.9 Å from RQ O1 and RQ O2, respectively), suggesting that electrons are first accepted by [3Fe–4S] upon the oxidization of RQH_2, and then transferred to FAD via [4Fe–4S] and [2Fe–2S].

RQ is surrounded by conserved amino acid residues (Ser C72, Arg C76, Asp D106 and Tyr D107) and is involved in hydrogen bond networks, RQ O1–Tyr D107–Arg C76–Asp D106 and RQ O2–Ser C72–RQ N–Arg C76–Asp D106. Protons abstracted from RQH_2 may leave along these networks. It should be noted that the amino group of RQ, which is replaced by the methoxy group in ubiquinone, is involved in one of the hydrogen bond networks.

In this study, the structure of *A. suum* QFR, the first structure of a mitochondrial QFR-type complex II, has been determined. A comparison of structures of *A. suum* QFR and SQR-type complex II reveals that not only are the protein structures essentially identical to each other, but also the bound prosthetic groups are surrounded by conserved residues (Fig. 1C). Thus, it appears that the bound quinone type plays a role in determining the direction of catalysis, QFR or SQR of complex II. In fact, *A. suum* QFR, which catalyses the reduction of fumarate ($Em' = +30\,mV$) by oxidizing RQH_2 ($Em' = -63\,mV$) *in vivo*, displays SQR activity,

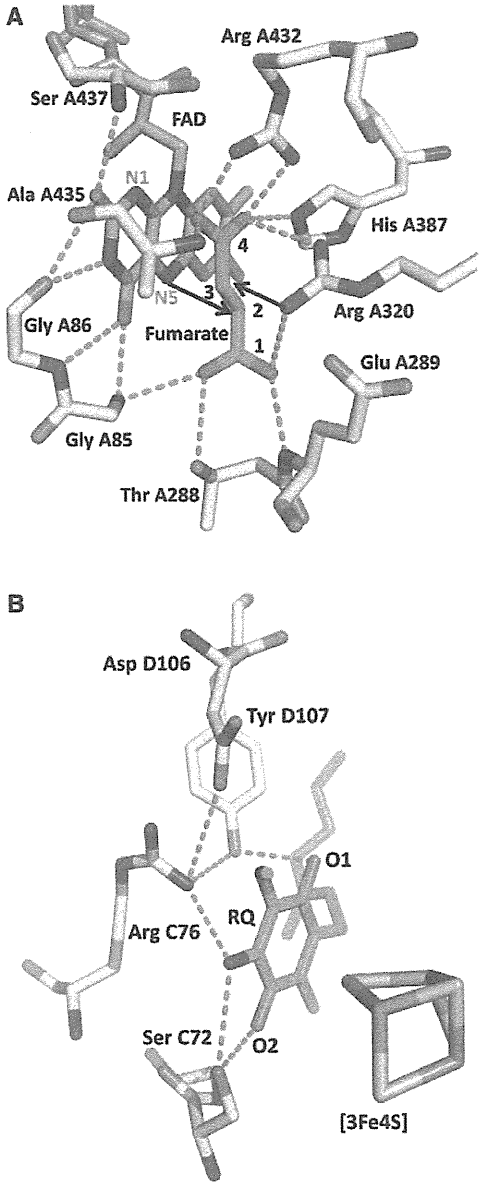

Fig. 2 Close-up views of active site structures of *A. suum* QFR. (A) Fumarate binding site of *A. suum* QFR. The C1 carboxyl group is twisted around the C1 and C2 bond by hydrogen bonds with nearby residues, which induces partial charge separation, $C2^{\delta+}$ and $C3^{\delta-}$. (B) RQH_2 binding site of *A. suum* QFR. Colour code for each atom type: C (yellow), N (blue), O (red), S (orange) and Fe (brown). Fumarate and RQ are coloured in green, FAD in pink. Hydrogen bonds are drawn with cyan dotted lines.

oxidation of succinate ($E_m' = +30$ mV), and reduction of ubiquinol ($E_m' = +110$ mV) *in vitro*.

The structure also demonstrates a feature unique to *A. suum* QFR. The additional polypeptide composed of 27 residues, which is found only at the N-terminus of *A. suum* CybS, extends to and forms hydrogen bonds with CybL, Ip and Fp (Fig. 1B, cyan), indicating that this unique region probably contributes to the stabilization of the *A. suum* QFR structure. In addition, because no such region has been found in SQR-type complex IIs known to date, this unique feature could make *A. suum* QFR favourable for accepting RQH_2 and fumarate as substrates, although further biochemical and biophysical analyses are necessary to reveal the truth.

Supplementary Data

Supplementary Data are available at *JB* Online.

Funding

This work was supported in part by Creative Scientific Research Grant 18GS0314 (to KK), Grant-in-aid for Scientific Research on Priority Areas 18073004 (to KK) and 19036010 (to SH) from the Japanese Society for the Promotion of Science, and Targeted Proteins Research Program (to KK and SH) from the Japanese Ministry of Education, Science, Culture, Sports and Technology (MEXT).

Conflict of interest

None declared.

References

1. Omura, S., Miyadera, H., Ui, H., Shiomi, K., Yamaguchi, Y., Masuma, R., Nagamitsu, T., Takano, D., Sunazuka, T., Harder, A., Kolbl, H., Namikoshi, M., Miyoshi, H., Sakamoto, K., and Kita, K. (2001) An anthelmintic compound, nafuredin, shows selective inhibition of complex I in helminth mitochondria. *Proc. Natl. Acad. Sci. USA* **98**, 60–62
2. Matsumoto, J., Sakamoto, K., Shinjyo, N., Kido, Y., Yamamoto, N., Yagi, K., Miyoshi, H., Nonaka, N., Katakura, K., Kita, K., and Oku, Y. (2008) Anaerobic NADH-fumarate reductase system is predominant in the respiratory chain of *Echinococcus multilocularis*, providing a novel target for the chemotherapy of alveolar echinococcosis. *Antimicrob. Agents Chemother.* **52**, 164–170
3. Sakai, C., Tomitsuka, E., Esumi, H., Harada, S., and Kita, K. (2012) Mitochondrial fumarate reductase as a target of chemotherapy: from parasites to cancer cells. *Biochim. Biophys. Acta* **1820**, 643–651
4. Sun, F., Huo, X., Zhai, Y., Wang, A., Xu, J., Su, D., Bartlam, M., and Rao, Z. (2005) Crystal structure of mitochondrial respiratory membrane protein complex II. *Cell* **121**, 1043–1057
5. Huang, L.S., Sun, G., Cobessi, D., Wang, A.C., Shen, J.T., Tung, E.Y., Anderson, V.E., and Berry, E.A. (2006) 3-Nitropropionic acid is a suicide inhibitor of mitochondrial respiration that, upon oxidation by complex II, forms a covalent adduct with a catalytic base arginine in the active site of the enzyme. *J. Biol. Chem.* **281**, 5965–5972
6. Yankovskaya, V., Horsefield, R., Tornroth, S., Luna-Chavez, C., Miyoshi, H., Leger, C., Byrne, B., Cecchini, G., and Iwata, S. (2003) Architecture of succinate dehydrogenase and reactive oxygen species generation. *Science* **299**, 700–704
7. Iverson, T.M., Luna-Chavez, C., Cecchini, G., and Rees, D.C. (1999) Structure of the *Escherichia coli* fumarate reductase respiratory complex. *Science* **284**, 1961–1966
8. Lancaster, C.R., Kroger, A., Auer, M., and Michel, H. (1999) Structure of fumarate reductase from *Wolinella succinogenes* at 2.2 Å resolution. *Nature* **402**, 377–385
9. Osanai, A., Harada, S., Sakamoto, K., Shimizu, H., Inaoka, D.K., and Kita, K. (2009) Crystallization of mitochondrial rhodoquinol-fumarate reductase from the parasitic nematode *Ascaris suum* with the specific inhibitor flutolanil. *Acta Crystallogr. Sect. F Struct. Biol. Cryst. Commun.* **65**, 941–944
10. Otwinowski, Z. and Minor, W. (1997) Macromolecular crystallography part A [20] Processing of X-ray diffraction data collected in oscillation mode. *Methods Enzymol.* **276**, 307–326
11. Vagin, A. and Teplyakov, A. (2010) Molecular replacement with *MOLREP*. *Acta Crystallogr. D Biol. Crystallogr.* **66**, 22–25
12. Murshudov, G.N., Vagin, A.A., and Dodson, E.J. (1997) Refinement of macromolecular structures by the maximum-likelihood method. *Acta Crystallogr. D Biol. Crystallogr.* **53**, 240–255
13. Emsley, P. and Cowtan, K. (2004) *Coot*: model-building tools for molecular graphics. *Acta Crystallogr. D Biol. Crystallogr.* **60**, 2126–2132
14. DeLano, W.L. (2002) *The PyMOL Molecular Graphics System*. DeLano Scientific LLC, Palo Alto, California, USA
15. Horsefield, R., Iwata, S., and Byrne, B. (2004) Complex II from a structural perspective. *Curr. Protein Pept. Sci.* **5**, 107–118
16. Page, C.C., Moser, C.C., Chen, X., and Dutton, P.L. (1999) Natural engineering principles of electron tunnelling in biological oxidation-reduction. *Nature* **402**, 47–52
17. Tomasiak, T.M., Archuleta, T.L., Andrell, J., Luna-Chavez, C., Davis, T.A., Sarwar, M., Ham, A.J., McDonald, W.H., Yankovskaya, V., Stern, H.A., Johnston, J.N., Maklashina, E., Cecchini, G., and Iverson, T.M. (2011) Geometric restraint drives on- and off-pathway catalysis by the *Escherichia coli* menaquinol:fumarate reductase. *J. Biol. Chem.* **286**, 3047–3056
18. Inaoka, D.K., Sakamoto, K., Shimizu, H., Shiba, T., Kurisu, G., Nara, T., Aoki, T., Kita, K., and Harada, S. (2008) Structures of *Trypanosoma cruzi* dihydroorotate dehydrogenase complexed with substrates and products: atomic resolution insights into mechanisms of dihydroorotate oxidation and fumarate reduction. *Biochemistry* **47**, 10881–10891

J. Biochem. 2012;152(3):259–268 doi:10.1093/jb/mvs058

JB THE JOURNAL OF BIOCHEMISTRY

Critical roles of the mitochondrial complex II in oocyst formation of rodent malaria parasite *Plasmodium berghei*

Received May 1, 2012; accepted May 16, 2012; published online May 23, 2012

Akina Hino[1,*], Makoto Hirai[2,3,*†], Takeshi Q. Tanaka[1,‡], Yoh-ichi Watanabe[1], Hiroyuki Matsuoka[3] and Kiyoshi Kita[1,§]

[1]Department of Biomedical Chemistry, Graduate School of Medicine, The University of Tokyo, 7-3-1 Hongo, Bunkyo-ku, Tokyo 113-0033, Japan; [2]Department of Parasitology, Graduate School of Medicine, Gunma University, 3-39-22 Maebashi City, Gunma 371-8511, Japan and [3]Division of Medical Zoology, Department of Infection and Immunity, School of Medicine, Jichi Medical University, Shimotsuke City, Tochigi 329-0498, Japan

*These authors contributed equally to this study.

†Makoto Hirai, Department of Parasitology, Graduate School of Medicine, Gunma University, 3-39-22 Maebashi City, Gunma 371-8511, Japan. Tel: +81-27-220-8023, Fax: +81-27-220-8025, email: makotohirai@gunma-u.ac.jp

‡Present address: Laboratory of Malaria and Vector Research, National Institute of Allergy and Infectious Diseases, National Institutes of Health, Rockville, MD 20892, USA.

§Kiyoshi Kita, Department of Biomedical Chemistry, Graduate School of Medicine, The University of Tokyo, 7-3-1 Hongo, Bunkyo-ku, Tokyo 113-0033, Japan. Tel: +81-3-5841-3528, Fax: +81-3-5841-3444, email: kitak@m.u-tokyo.ac.jp

It is generally accepted that the mitochondria play central roles in energy production of most eukaryotes. In contrast, it has been thought that *Plasmodium* spp., the causative agent of malaria, rely mainly on cytosolic glycolysis but not mitochondrial oxidative phosphorylation for energy production during blood stages. However, *Plasmodium* spp. possesses all genes necessary for the tricarboxylic acid (TCA) cycle and most of the genes for electron transport chain (ETC) enzymes. Therefore, it remains elusive whether oxidative phosphorylation is essential for the parasite survival. To elucidate the role of TCA metabolism and ETC in malaria parasites, we deleted the gene for flavoprotein (Fp) subunit, *Pbsdha*, one of four components of complex II, a catalytic subunit for succinate dehydrogenase activity. The Pbsdha(-) parasite grew normally at blood stages in mouse. In contrast, ookinete formation of Pbsdha(-) parasites in the mosquito stage was severely impaired. Finally, Pbsdha(-) ookinetes failed in oocyst formation, leading to complete malaria transmission blockade. These results suggest that malaria parasite may switch the energy metabolism from glycolysis to oxidative phosphorylation to adapt to the insect vector where glucose is not readily available for ATP production.

Keywords: complex II/malaria parasite/mitochondria/*Plasmodium berghei*.

Abbreviations: AP, alkaline phosphatase; BCIP, 5-bromo-4-chloro-3'-indolylphosphatase *p*-toluidine salt; Cyt *b*, cytochrome *b*; Cyt *c*, cytchrome *c*; DHOD, dihydroorotate dehydrogenase; ETC, electron transport chain; FAD, flavin adenine dinucleotide; FBS, fetal bovine serum; Fp, flavoprotein; FRD, fumarate reductase; HRP, horse radish peroxidase; Ip, iron–sulphur cluster protein; MQO, malate–quinone oxidoreductase; MV, methylviologen; NAD, nicotineamide adenine dinucleotide; NBT, nitroblue tetrazolium chloride; NDH2, type2 NADH–ubiquinone oxidoreductase; Q, quinine; QFR, quinol–fumarate reductase; SDH, succinate dehydrogenase; SQR, succinate–ubiquinone reductase; TBS, tris buffered saline; TCA, tricarboxylic acid.

Malaria is one of the most serious diseases in the world. It causes one million infant deaths and over 500 million clinical cases annually, of which 85% is in sub-Saharan Africa (*1*). The drugs such as pyrimethamine/sulphadoxine, chloroquine or artesunate are the common treatment against malaria, but there is the emergence and spread of drug-resistant malaria parasites throughout the world (*2*), resulting in an urgent need for new drug.

The mitochondrion of *Plasmodium* species is obvious target of antimalarial drugs, but the physiological importance of this organelle is poorly understood. In other eukaryotes, pyruvate dehydrogenase is localized in mitochondria where it links the glycolysis metabolic pathway to TCA cycle, while it is localized in the apicoplast in *P. falciparum* (*3*). Therefore, it has been unclear until recently how glycolysis metabolism is connected to the tricarboxylic acid (TCA) cycle. Blood-stage *P. falciparum* have only a single mitochondrion without crista (*4*). Such morphologically immature mitochondrion suggests that, unlike other eukaryotes, the blood stage *P. falciparum* relies mainly on cytoplasmic glycolysis for their energy metabolism but not on mitochondrial oxidative phosphorylation (*5*, *6*). Beside, recent omics-based studies showed that *P. falciparum* expressed all TCA cycle enzyme genes and most ones for the electron transport chain (ETC), and that *P. falciparum* produced the intermediates of the TCA cycle (*7*). Moreover, the genes for TCA cycle are upregulated at mosquito stages (*8*). The gametocytes, precursor cells of gametes possess mitochondria with cristae (*9*). These data suggest that mitochondrial energy metabolism may have more crucial roles in insect stages than blood stages,

which have not been intensively investigated until recently.

The mitochondrial complex II (succinate–ubiquinone reductase: SQR) oxidizes succinate to produce fumarate as a TCA cycle member enzyme. In the anaerobic electron transfer system, complex II carries out fumarate reduction using quinol as an electron donor (quinol–fumarate reductase; QFR), which is the reverse reaction of SQR. Complex II consists of four subunits, flavoprotein (Fp), iron–sulphur cluster protein (Ip) and two small membrane anchor subunits, cytochrome *b* large (CybL) and small (CybS) subunits. The Fp with molecular mass of 70 kDa has a flavin adenine dinucleotide (FAD) covalently bound to a highly conserved histidine (His) residue. Fp and Ip form catalytic portion of the complex and this portion acts as a succinate dehydrogenase (SDH), catalyzing the oxidation of succinate by water-soluble electron acceptors such as phenazine methosulphate in SQR, while it acts as a fumarate reductase (FRD), catalyzing electron transfer from water-soluble electron donors such as reduced methylviologen (MV) to fumarate in QFR. FAD in the Fp receives the reducing equivalents from succinate and then transfers it to quinone by SQR activity where the two small membrane anchor subunits are indispensable (*10*). Thus, complex II functions as a link between the TCA cycle and the ETC, directly. While complex II has such critical roles in energy metabolisms, and Fp and Ip subunits genes are substantially conserved in various organisms (*3*, *11*), two small membrane anchor subunit genes are diverse and had not been detected in the genomes of *Plasmodium* spp., suggesting that plasmodial complex II is nonfunctional. However, recently our intensive database mining has identified putative plasmodial anchor subunit genes (*12*). Moreover, biochemical studies revealed that SQR activity of complex II was detected in the mitochondrial fraction of *P. yoelii* and *P. falciparum*, and the activity was inhibited by the ubiquinone-binding site inhibitor, atopenin A5 (*13–15*).

In this work, we took genetic approach to understand the physiological role of the parasite complex II using *P. berghei* as a model because the whole parasite life cycle can be monitored using mosquito and mouse as hosts. We generated transgenic *P. berghei* (Pbsdha(-)) in which the Fp subunit gene (*Pbsdha*) of complex II was deleted to inactivate complex II activities. By infecting mice and mosquitoes with the Pbsdha(-) parasites, we followed phenotype of the Pbsdha(-) parasite during the whole life cycle and found that complex II is essential for oocyst formation in the mosquito.

Materials and Methods

Maintenance of mosquitoes and parasites

Anopheles stephensi (SDA 500 strain) and *P. berghei* (ANKA clone 2.34) were maintained as described previously (*16*). *P. berghei*-infected mosquitoes were fed on naïve mice (Balb/c), and the resulting infected mice were referred to as passage 0 (P0). The P0 blood was injected intraperitoneally to the naïve mice and the passage one (P1) mice were used in the experiments. The experiments using animals and recombinant DNA were performed under the guidelines of the committee in Jichi University, and assigned permission no. is 08-14.

Generation of Pbsdha::AGFP parasites

The two fragments covering the 5'UTR and the first 60 amino acids (−3229 to +180 bp), and 3' UTR (1025 bp) of *Pbsdha* gene (PBANKA_051820) were amplified with primer pairs 5'UTRB4F/5'UTRB1R and 3'UTRB2F/3'UTRB3R, and *P. berghei* genomic DNA as template. The *Azami Green Fluorescent Protein* gene (*AGFP*) was amplified with the primers AzamiB1F/AzamiB2R. Each PCR fragment was cloned into *pDONRP4-P1R*, *P1-P2R* and *P2-P3R* vectors by BP clonase reaction (Invitrogen) to generate entry vectors (*5UTR/P4P1*, *AGFP/P1P2* and *3UTR/P2P3*). An R4-R3 fragment (Invitrogen) was inserted into *HindIII* site of *pBS-DHFR* vector (*17*) to generate an acceptor plasmid (*R4R3/pBS-DHFR*). The inserts of entry vectors were transferred to the acceptor plasmid by LR reaction using the Multisite Gateway Three-Fragment Vector Construction Kit (Invitrogen). In the final plasmid (*Pbsdha::AGFP*), 5' UTR and the first 60 amino acids of *Pbsdha* were fused to the *AGFP* gene. Thus, the expression of the *AGFP* reporter gene is under the control of the *Pbsdha* gene promoter. For parasite transfection, the plasmid was digested by *BstXI*, and the linearized plasmid was integrated into the parasite genome by single crossover homologous recombination. The parasite transfection and subsequent cloning were performed as described elsewhere (*18*). Correct integration events in Pbsdha::AGFP parasites clones were confirmed by Southern blot as described later in the text. The genomic DNA (10 μg) of Wild Type (WT) and Pbsdha::AGFP parasites was digested with *PacI* and *HpaI*, separated by 0.8% (w/v) agarose gel and transferred to the Hybond-N+ membrane (GE healthcare). PCR fragment (F1-HindIII/R1-HindIII) was labeled with AlkPhos Direct Labeling Reagent Kit (GE Healthcare) and used as probe for hybridization. The hybridization and washing were performed by following the manufacturer's protocol.

The expression of the AGFP gene at each developmental stage in Pbsdha::AGFP parasites was investigated as follows. To prepare the parasites at blood stages, the mouse blood (1 ml) infected with Pbsdha::AGFP parasites was collected, mixed with 120 ml RPMI1640 containing 25% fetal bovine serum (FBS) and cultured at 37°C for 16 hr by the candle-jar method (*19*). The parasites synchronized to schizonts were partially purified by Nycoprep 1.077 (*18*) and injected intravenously into mice tail veins. At 4 hr and 33 hr after injection, the parasites were synchronized to ring and trophozoite stages, respectively. A drop of tail blood was collected at these time points, and the AGFP signal in rings, trophozoites, and *in vitro* cultured schizonts was observed. For the analysis of AGFP expression in mosquito-stage parasites, the ookinetes were prepared *in vitro* as described in 'Examination of Pbsdha(-) parasite development'. The mosquitoes were fed on mice carrying Pbsdha::AGFP parasites and dissected on day 14 and 16 after the feeding. The AGFP signal in the oocysts (on midguts) and sporozoites (in salivary glands) as well as *in vitro*-cultured ookinetes was observed. The parasite was stained with 10 nM of MitoTracker Orange CMTM Ros (Molecular Probes) and DAPI (4',6-diamino-2-phenylindole) (Dako) to label mitochondria and nuclei, respectively. The fluorescent signal of MitoTracker, DAPI and AGFP was detected at 540 nm, 452 nm and 520 nm, respectively.

Targeted disruption of the Pbsdha gene

Two regions of the *Pbsdha* gene were amplified by PCR using primer pairs F1-HindIII/R1-HindIII and F2-EcoRI/R2-BamHI, and *P. berghei* genomic DNA as template. The PCR fragments were digested with respective restriction enzymes and cloned to *pBS-DHFR* to give a targeting plasmid, *pPbsdha(-)*. The *pPbsdha(-)* plasmid was digested with *ClaI* and *BamHI*, and the plasmid was introduced in *P. berghei* by electroporation. The correct recombination event of the clones was confirmed by diagnostic PCR using two primer sets, K1 (K1-F and R) and K2 (K2-F and R). Correct integration was also checked by Southern blot analysis as described earlier in the text. The genomic DNA of WT and Pbsdha(-) parasites was digested with *PacI*, and a PCR fragment (F1-HindIII/R1-HindIII) was used as probe. The contamination of WT parasites in Pbsdha(-) parasite clone was checked by PCR with primer set W (W-F and R). Two clones from two independent transfection experiments were isolated and analyzed further. All primer sequences are described in supplementary information.

Western blot analysis of mitochondrial fraction

The mitochondrial fractions were prepared from mouse leucocytes, *in vitro* cultured *P. falciparum*, and WT and Pbsdha(-) of *P. berghei* by N_2 cavitation methods (*13*, *14*). The mitochondrial fractions of mouse liver (10 μg/lane), WT and Pbsdha(-) of *P. berghei* (20 μg/lane) and *P. falciparum* (10 μg/lane) were loaded onto 10% SDS polyacrylamide gel electrophoresis and transferred to a nitrocellulose membrane (Whatman). The membrane was blocked with SuperBlock (Pierce) and washed with TBS-T (150 mM NaCl, 0.05% (v/v) Tween 20, 10 mM Tris-HCl; pH 7.5). To detect the Fp subunit, the membrane was hybridized with antiserum against the *P. falciparum* Fp peptide (*20*) as primary antibody (1/1,000 dilution) and alkaline phosphatase (AP) conjugated anti-rabbit IgG antiserum as secondary antibody (1/10,000 dilution). The AP enzyme activity on the membrane was visualized by a chromogenic method using NBT and BCIP. To confirm the equal loading of the samples on the gel, *P. berghei* heat shock protein 70 (HSP70) was used as internal control. The same membrane used in Fp detection was rehybridized with anti-HSP70 antiserum as primary antibody (1/100 dilution) and horse radish peroxidase (HRP) conjugated anti-mouse IgG antiserum as secondary antibody (1/10,000 dilution). HRP enzyme activity was detected as chemiluminescent signal by the Immobilon Western Chemiluminescent HRP Substrate (Millipore).

Measurement of SQR activity in mitochondrial fraction

The SQR enzyme activity assay was performed at 25°C with a V-660 spectrophotometer (JASCO, Tokyo, Japan). The enzyme activity of SQR was determined as quinone-mediated succinate: 2,4-dichlorophenolindophonol (DCIP) reductase in 30 mM Tris-HCl (pH 8.0) containing 10 mM potassium succinate, 100 μM ubiquinone-2 and 45 μM DCIP ($\varepsilon^{600nm} = 21\,mM^{-1}cm^{-1}$) in the presence of 2 mM KCN and 0.1 μM Atpenin A5 (Alexis Biochemicals). Atpenin A5 was proven to be a novel inhibitor specific to mouse leukocytes but not parasitic SQR activity at this concentration in our previous study (*13*).

Examination of Pbsdha(-) parasite development

To assess the growth rate of the parasites in mice, the red blood cells (RBC) (10^4) infected with either WT or Pbsdha(-) parasites were intravenously injected into tail vein of each of the four naïve mice. Subsequently, the tail blood was taken every 24 hr and the number of infected RBCs was counted. To investigate the male gametogenesis, the infected blood (10 μl) was added to 1 ml of fertilization medium (10 % (v/v) FBS in RPMI1640 (pH 8.2)) at 21°C. The sample (10 μl) was taken at 15 min and the number of exflagellating male gametes was counted. The rest of the sample was further incubated for 16 hr and the number of ookinetes was counted. The fertilization rate was calculated by the conversion rate of female gametocytes into ookinetes.

Infectivity of Pbsdha(-) parasite to mosquito and transmission to mouse

The tail blood of WT- and Pbsdha(-)-infected mice was taken and the number of exflagellating male gametes was counted. Only the mice whose blood contained over 2 exflagellating centers per 10^4 RBC were used for the mosquito feeding. Female mosquitoes (4–7 days old) were fed on the infected mice, and fully engorged mosquitoes were collected. Sixteen days after blood feeding, midguts and salivary glands were isolated. The number of oocysts in the midgut was counted and the presence of sporozoites in the salivary gland was examined to assess the infectivity of the parasites to mosquitoes. To investigate the transmission efficiency to mice, more than 20 mosquitoes carrying WT or Pbsdha(-) parasites were fed on naïve mice. The transmission of the parasites to mice was examined by checking mouse blood smears until 2 weeks after the mosquito feeding.

Results

Identification and expression analysis of Pbsdha

We found PBANKA_051820 being annotated as a putative Fp subunit gene of complex II in PlasmoDB, and hereafter it is referred to '*Pbsdha*'. It is known that amino acid sequences of Fp are highly conserved among various organisms. As such, the amino acid sequence of *P. berghei* FP (PbFp) shows high identity to those of other organisms including *P. falciparum* Fp, which we have reported previously (*11*). Especially, histidine in the FAD binding site in the catalytic domain is completely conserved in PbFp (Fig. 1).

To investigate *Pbsdha* gene expression during parasite life cycle, we generated Pbsdha::AGFP parasites as a reporter line, in which *AGFP* reporter gene expression is regulated by the endogenous *Pbsdha* gene promoter (Fig. 2A). It is reported that the first 60 amino acids of *P. falciparum* Fp (PfFp) contain a functional mitochondrial targeting signal (*21*) and the corresponding amino acid sequence of PbFp shows 75% identity to that of PfFp (*11*), suggesting the same function in the corresponding region of PbFp. To investigate the cellular localization and developmental expression of AGFP during the parasite life cycle, the first 60 amino acids of PbFp was fused to AGFP (Pbsdha::AGFP). The WT parasites were transfected with the *Pbsdha::AGFP* plasmid and the correct integration event in Pbsdha::AGFP parasite clone was confirmed by Southern blot (Fig. 2B). For the analysis of cellular localization of AGFP, the Pbsdha::AGFP parasites were stained with MitoTracker Orange to label the mitochondrion. As shown in Fig. 2C, AGFP signals colocalized with MitoTracker Orange signals, indicating that the N-terminal sequence of PbFp possesses a functional mitochondrial targeting signal. Next, we investigated the reporter gene expression at each developmental stage of parasites in red blood cell. AGFP signal was detected in trophozoite and schizont (Fig. 2D) but not in the ring form stage (data not shown). To investigate the AGFP expression in the parasites at mosquito stages, Pbsdha::AGFP parasites were fed to mosquitoes. As shown in Fig. 2E, the signal was detected in *in vitro*-cultured ookinetes, and oocysts and sporozoites in mosquitoes. These results indicate that *Pbsdha* was expressed in both blood stages and mosquito stages.

Disruption of the Pbsdha gene

Then, to study the *P. berghei* complex II functions, we generated Pbsdha(-) parasites by replacing the *Pbsdha* gene with *TgDHFR* (Fig. 3A). Two independent clones (KO-a and KO-b) were established by independent transfection experiments. The correct targeting event in each clone was confirmed by Southern blot analysis (Fig. 3B) and diagnostic PCR (Fig. 3C). Following the confirmation of *Pbsdha* gene disruption, we further checked the deletion of the PbFp protein and SQR enzyme activity in Pbsdha(-) parasites by Western blot and enzyme activity assay, respectively. For these experiments, we prepared the crude mitochondrial samples from WT, Pbsdha(-) parasites, *in vitro* cultured *P. falciparum*, and naïve mouse liver. To detect the Fp peptide by Western blot analysis, we used the anti-PfFp antiserum (*20*) because the amino acid sequence of PfFp shows high identity to those of PbFp (90.5 %) and mice Fp (63.3 %). It is thus anticipated that the antiserum may cross-react to both PbFp and mice Fp proteins. As shown in Fig. 3D, the antiserum reacted to the peptides with expected size of

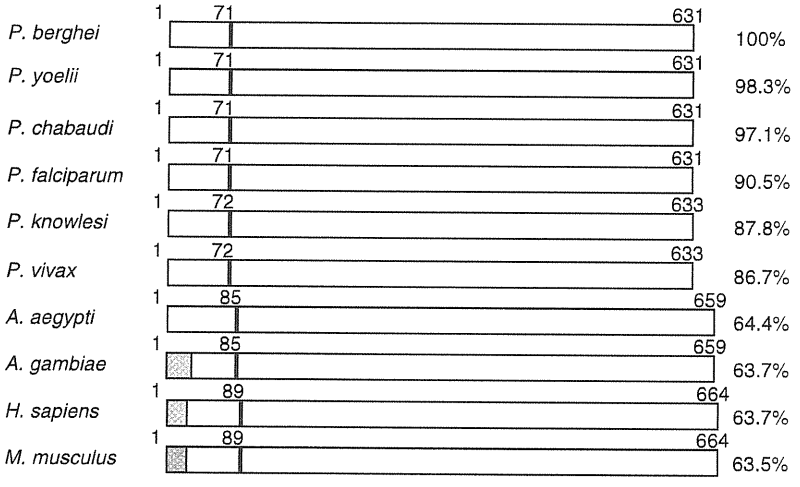

Fig. 1 Primary structure of Fp proteins from 10 species. The box indicates the full-length Fp protein. The mitochondrial sorting signal is colored in grey. The black line with number indicates the conserved His for FAD binding site. The total number of amino acid residues and the amino acid identity to PbFp are indicated on the right (%).

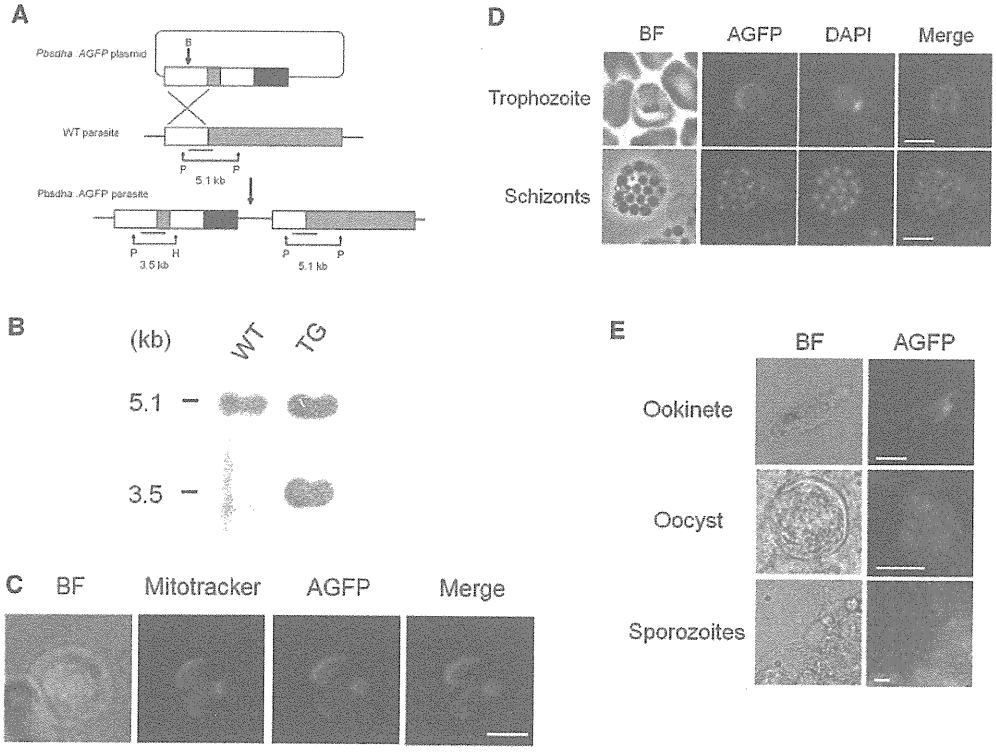

Fig. 2 Generation of the transgenic parasite line Pbsdha::AGFP. (A)Schematic representation of *AGFP* tagging of the *Pbsdha* locus using a plasmid that integrated through single crossover homologous recombination. In the *Pbsdha::AGFP* plasmid, the boxes indicate *Pbsdha* gene promoter (white), the first 60 amino acids of Pbsdha (dark gray), AGFP (light gray), 3′UTR of *Pbsdha* gene and *TgDHFR/ts* selectable marker cassette (black). In the *Pbsdha* gene locus (middle), the box with dark gray indicates full open reading frame of *Pbsdha*. B, H and P indicate *BstXI*, *HpaI* and *PacI* digestion sites, respectively. Bars represent the position of the probe used in Southern blot analysis. (B) Southern blot analysis of WT and Pbsdha::AGFP parasites. Hybridization of the probe with *PacI*- and *HpaI*-digested genomic DNA yielded a 5.1 kb for WT, and 3.5 kb and 5.1 kb for Pbsdha::AGFP parasites (TG). (C) Cellular localization of AGFP in Pbsdha::AGFP parasites. The mouse erythrocyte infected with Pbsdha::AGFP parasites was observed under bright field (BF). The signals of MitoTracker and AGFP in the same cell were detected through red (MitoTracker) and green filter (AGFP), respectively. Bar represents 5 μm. (D) Expression of *AGFP* gene in Pbsdha::AGFP parasites at blood stages. The AGFP signal was detected in the parasites synchronized at trophozoite (upper) and schizont stages (lower). Nuclei were stained with DAPI. Bars represent 5 μm. (E) Expression of the *AGFP* gene in Pbsdha::AGFP parasites at mosquito stages. The AGFP signal was detected in *in vitro* cultured-ookinetes, oocysts in the midguts and sporozoites in the salivary gland of mosquitoes. Bar represents 20 μm.

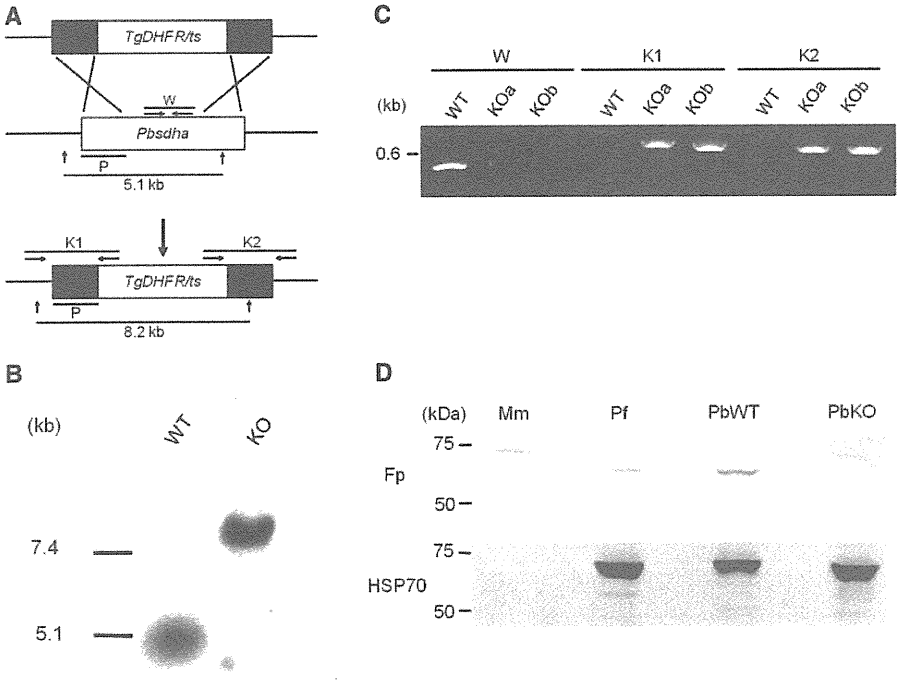

Fig. 3 Targeted disruption of the *Pbsdha* gene. (A) Schematic representation of the replacement strategy to generate Pbsdha(-) parasites. The WT *Pbsdha* gene locus is replaced with 5′ and 3′ UTRs of the *Pbsdha* gene and *TgDHFR*, a selectable marker. Vertical arrows indicate *PacI* site. P with bar indicates the probe position for Southern blot analysis. Arrows marked with W (WT specific) or K1/K2 (knockout specific) indicate the primer positions used in diagnostic PCR. (B) Southern blot genotyping confirmed integration. Hybridization of the probe with *PacI*-digested genomic DNA of WT and Pbsdha(-) parasites yielded a 5.1 kb and 8.2 kb band, respectively. (C) Confirmation of *Pbsdha* gene disruption by diagnostic PCR. Genomic DNA from WT, Pbsdha(-) clone A (KOa) and clone B (KOb) were used as templates. The positions of the PCR products in W and K1/K2 are depicted in Fig. 2A. (D) Detection of Fp peptides by Western blot analysis. The Fp peptides in mitochondrial fractions of *Mus musculus* (Mm), *P. falciparum*(Pf), *P. berghei* wild-type (PbWT) and Pbsdha(-) (PbKO) parasites were detected by anti-PfFp antiserum (upper panel). The anti-PbHSP70 antiserum was used to confirm equal loading of the protein samples in each lane (lower panel).

70.5 kDa (WT *P. berghei*) and 73.0 kDa (mice), as well as 70.7 kDa (*P. falciparum*). In contrast, no band was detected in Pbsdha(-) (PbKO) except for the high molecular weight band, which is speculated as contaminated mice Fp because the molecular weight of this faint band is similar to that of the band on Mm lane (Fig. 3D). The equal loading of each sample on the gel was confirmed by anti-PbHSP70 antiserum (lower panel in Fig. 3D). These results demonstrated that the PbFp protein was surely deleted from Pbsdha(-) parasites. Next, we investigated the SQR activity in Pbsdha(-) parasites by using the same samples used for Western blot analysis. While WT parasites showed an SQR activity of 4.38 ± 0.96 nmol/min/mg ($N = 3$), Pbsdha(-) did not show any detectable SQR activity (Table I). These results demonstrated that the PbFp protein and the SQR activity were completely eliminated from the Pbsdha(-) parasites.

Phenotypic analysis of Pbsdha(-) parasites

As the disruption of the *Pbsdha* gene was confirmed, phenotypic effect of the gene disruption on the parasite was analyzed. In erythrocytic stages, Pbsdha(-) parasites underwent normal development and differentiation into gametocytes, which were not significantly different from those of WT parasites ($P > 0.1$, Fig. 4 and Table II). Successful *Pbsdha* gene deletion indicates that the SQR enzyme is not essential for the survival of the parasite at asexual stages and sexual differentiation. The mitochondria of Pbsdha(-) parasites were stained with Mitotracker, indicating that disruption of *Pbsdha* did not affect the mitochondrial membrane potential (Fig. 5).

Next, we investigated the parasite development at mosquito stages. In *P. berghei*, an *in vitro* assay has been established that mimics the gametogenesis and fertilization taking place in the mosquito body (*22*). Using this system, we confirmed that the efficiency of male gametogenesis in Pbsdha(-) parasites was comparable with that of WT parasites (data not shown). However, Pbsdha(-) parasites showed severe defects in ookinete formation, the stage next to fertilization. The conversion rate of female gametes to ookinetes in Pbsdha(-) was significantly reduced to 17% of WT parasite ($P < 0.05$ ($N = 3$), Fig. 6A). We further investigated the infectivity of Pbsdha(-) parasites to mosquitoes and the subsequent transmission to mice. The mosquitoes were fed on mice carrying either Pbsdha(-) or WT parasites, and then these mosquitoes were dissected for the evaluation of parasite development at day 16 post-feeding. Interestingly, several independent experiments using two clones showed that no oocysts were detected in the midguts of mosquitoes fed on mice carrying Pbsdha(-) parasites, while oocysts

Table I. SQR activity of the mitochondrial fraction in WT and Pbsdha(-) parasites.

	Exp 1	Exp 2	Exp 3
WT	5.31	4.44	3.40
KO	0.00	0.00	0.00

The value represents SQR activity in each independent assay (nmol/min/mg protein)

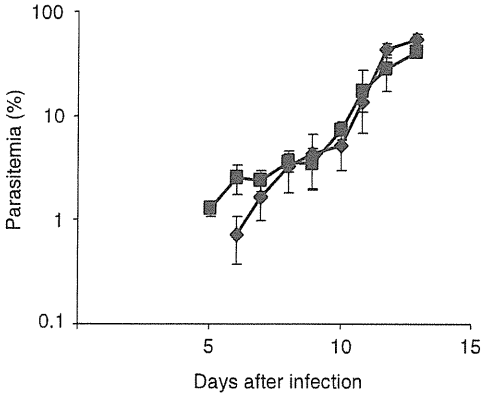

Fig. 4 The growth rate of intraerythrocytic stages of WT and Pbsdha(-) parasites. The parasitemia of WT and Pbsdha(-) parasites are indicated by closed square and diamond, respectively. Bar represents SD (N = 4).

Table II. The gametocytemia of WT and Pbsdha(-) parasites.

Parasites	Macrogametocytemia/ parasitemia	Microgametocytemia/ parasitemia
WT	6.5 ± 2.72	1.7 ± 0.45
KO	5.0 ± 1.11	1.5 ± 0.64

were detected in the mosquitoes fed on mice carrying WT parasites (Fig. 6B). Moreover, no transmission was observed in the mice challenged by the mosquitoes carrying Pbsdha(-) parasites, while WT parasites were transmitted to mice (Table III). Taken together, these results indicated that the development of Pbsdha(-) parasites was completely halted at the stage of oocyst formation.

Discussion

It is known that asexual stages parasites possess a single acristate mitochondria, while gametocytes, mosquito stages and preerythrocytic stage parasites possess five to six cristate mitochondria (*9*, *23*). This morphological maturation of mitochondria in the sexual stage parasites may correlate with the increased need of mitochondrial metabolism in the insect stage parasite development. Once malaria parasites are introduced to mosquitoes, they encounter to drastic environmental changes where the main sugar source is changed from glucose to torehalose, and they need to adapt to this (*24*). Our present work clearly shows that complex II has a critical role in parasite adaptation to the insect body. Namely, the parasite lacking complex II activity failed to form oocysts in mosquitoes, while the development of blood stage parasites in mice was not affected by *Pbsdha* gene disruption at all.

Developmental expression and targeting disruption of Pbsdha gene

By using Pbsdha::AGFP parasites as a reporter, we followed the AGFP expression during the whole parasite life cycle except for liver stage. Except for the ring stage, AGFP signals were detected in all developmental stages. It was reported that the size and morphology of mitochondria spectacularly changes during the life cycle and that the mitochondrial size is much smaller in the ring stage than in any other stage (*25*). Thus, the failure of signal detection in ring stage could be attributed to lower signal strength than the detection limit. According to gene expression data in PlasmoDB, the *P. falciparum* orthologous gene of *Pbsdha*, PF10_0334 is substantially expressed in all developmental stages including the ring form. Taken together, it can therefore be speculated that the *Pbsdha* gene is also expressed in all developmental stages.

In a global gene expression analysis, it was reported that several lines of *in vitro*-cultured *P. falciparum* showed very similar pattern in gene expression. In contrast, it was recently demonstrated that parasites derived directly from infected patients showed three distinct gene expression states (*26*). One of these states showed that the expression levels of *sdha* and other TCA cycle- or ETC-related genes are increased. Because such expression state has never been detected in *in vitro* studies and parasitic mitochondria are immature acristates, it had been considered that the blood-stage parasites mainly use cytosolic glycolysis and mitochondrial oxidative phosphorylation only marginally (Fig. 7). The discrepancy between the *in vivo* and *in vitro* studies above suggests that the parasites may use oxidative phosphorylation in *in vivo* in case that the patient would be hypoglycemic, which is reflected in the upregulation of the genes involved in oxidative phosphorylation. In the *in vitro* system, on the other hand, glucose is continuously supplied in the medium and the environmental condition is artificially controlled, therefore the parasites may exclusively undergo glycolysis and the enzymes of oxidative phosphorylation may be marginally expressed. Thus, it is important to undertake experiments using both *in vitro* and *in vivo* systems in order to understand how parasites respond to various environmental stimuli. In this sense, the rodent malaria model could be an ideal tool to investigate the changes in parasite metabolism *in vivo*.

Complex II is essential for the parasite survival at mosquito stages

We successfully generated Pbsdha(-) parasites, confirmed by Southern blot, diagnostic PCR and SQR activity assay. It is anticipated that the mitochondrial membrane potential was decreased in Pbsdha(-) parasites as a result of the knockout. Unexpectedly, the

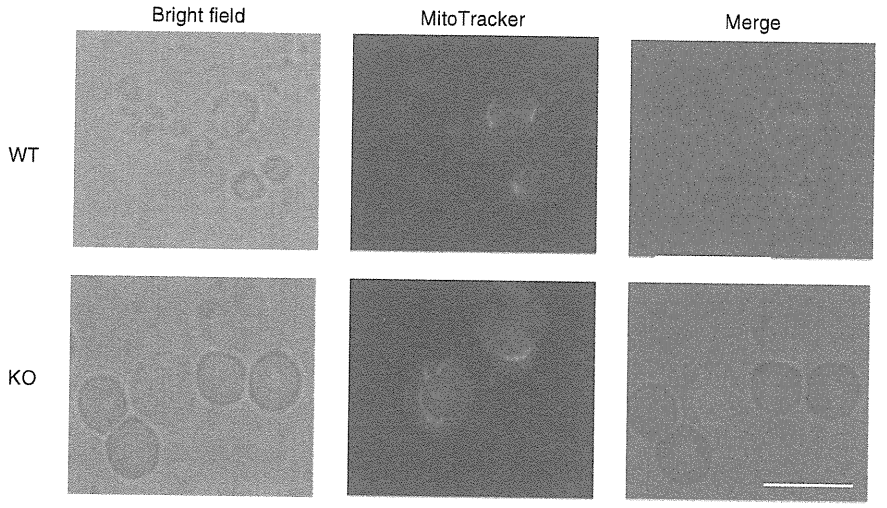

Fig. 5 MitoTracker staining of WT and Pbsdha(-) parasites. The erythrocytes infected with WT or Pbsdha(-) (KO) parasites was stained with MitoTracker to assess the integrity of the mitochondrial membrane potential. Bar represents 5 μm.

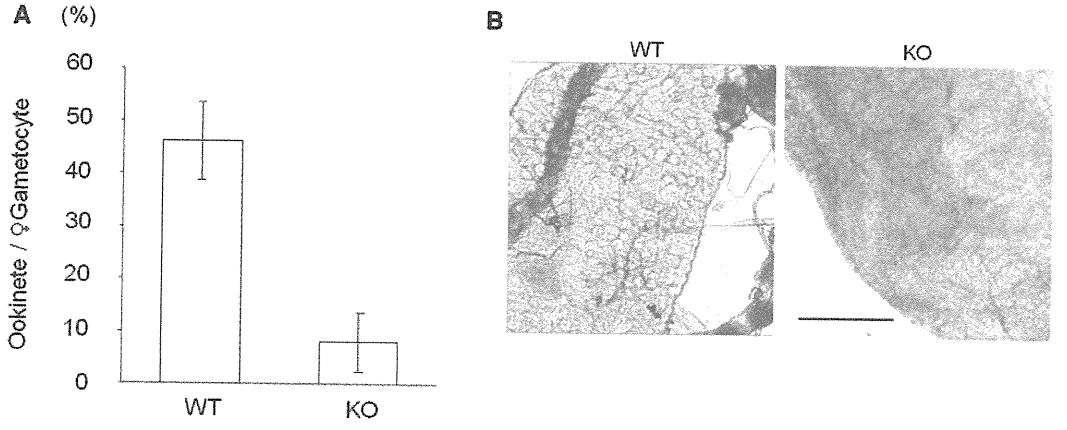

Fig. 6 Phenotypic analysis of Pbsdha(-) parasites. (A) Ookinete formation rate of WT and Pbsdha(-) (KO) parasites. The mouse blood infected with either WT or Pbsdha(-) parasites was incubated in fertilization medium to induce fertilization and differentiation into ookinetes. The ookinete formation rate was calculated by the percentage of female gametocytes, which converted into ookinetes. Error bars represents mean ± SD (n = 3). (B) Mosquito midguts infected with WT and Pbsdha(-) (KO) parasites. The latter carries no oocyst. Bars represent 200 μm.

Table III. Infectivity of WT and Pbsdha(-) parasites.

Parasite		Oocyst-positive mosquitoes	Mean oocysts/ midgut ± SD	Mouse infection
WT	Exp1	7/21	5.4 ± 11.3	+
	2	6/20	7.3 ± 6.4	+
	3	5/20	18.0 ± 30.3	+
	4	13/20	25.1 ± 30.5	+
	5	15/32	51.8 ± 63.4	+
Koa	Exp1	0/20	0	−
	2	0/20	0	−
	3	0/20	0	−
	4	0/20	0	−
	5	0/20	0	−
	6	0/20	0	−
Kob	Exp1	0/26	0	−

mitochondrial membrane potential seemed to be maintained in blood-stage parasites in the absence of complex II, which was demonstrated by the positive signal in MitoTracker staining. In addition to complex II, there are three other enzymes involved in electron flux that contribute to mitochondrial membrane potential; MQO (malate–quinone oxidoreductase), DHOD (dihydroorotate dehydrogenase) and NDH2 (type2 NADH–ubiquinone oxidoreductase), which is a single peptide dehydrogenase different from multi-subunit complex I (Fig. 7). It is therefore conceivable that any of these three enzymes may be a functional complement for the absence of complex II. Recently, it was reported that *P. berghei* lacking NDH2 (NDH2(-)) did keep mitochondrial membrane potential (*27*), supporting the hypothesis of mutual complementation among ETC enzymes.

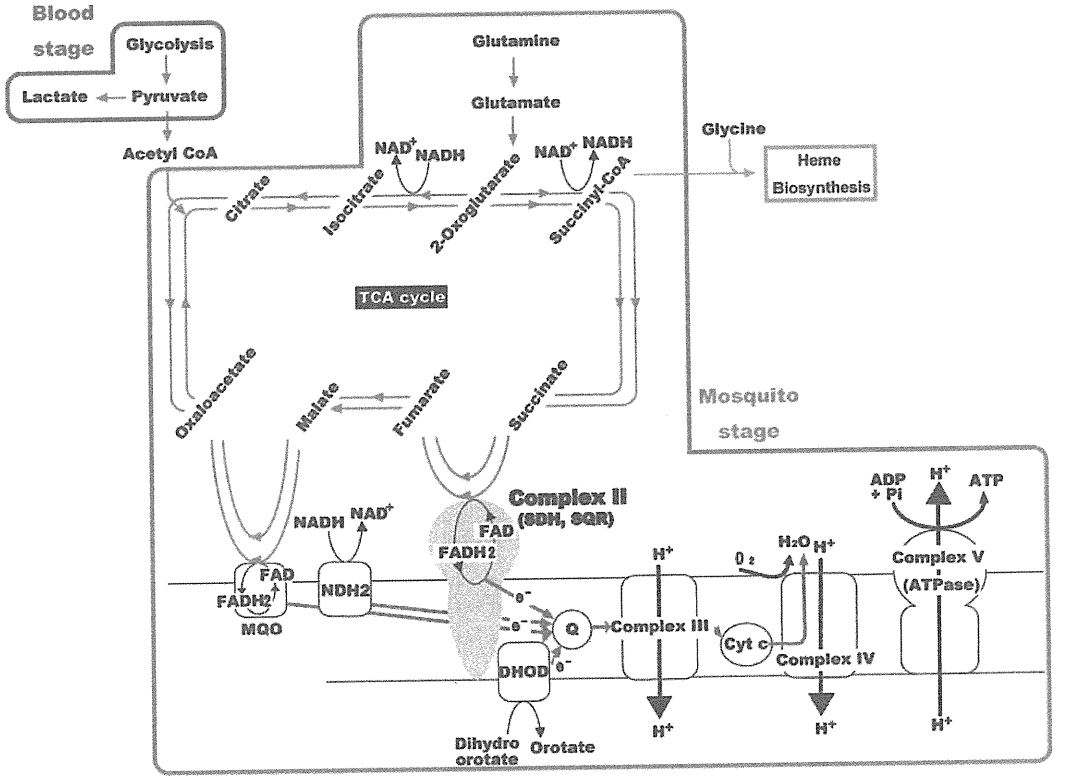

Fig. 7 Hypothetical Model of Plasmodial energy metabolism. Blue arrows represent canonical flow of glycolysis and TCA cycle. Green arrows represent *Plasmodium* TCA metabolism pathway. Unlike other eukaryotes, glycolysis (enclosed by red) does not link to TCA cycle. *Plasmodim* TCA cycle is initiated by uptaking of glutamine into mitochondria. Mitochondrial oxidative phosphorylation (enclosed by green) is essential for the parasite survival at mosquito stage because the Pbsdha(-) parasite is lethal at this stage.

Our phenotypic study revealed that Pbsdha(-) parasites proliferated and produced gametocytes with a similar rate to WT parasites in mice. Recently, we observed similar results in the blood-stage *P. falciparum*, of which Fp subunit was disrupted (Tanaka *et al.*, submitted for publication). *In vitro*, Pbsdha(-) male gametocytes differentiated to gametes (exflagellated) as WT ones, suggesting that complex II is not required for those developmental stages. It is known that mammalian sperm requires ATP for flagellum movement, which is supplied mainly from mitochondrial oxidative phosphorylation (*28*). While male gametes of malaria parasites show similar motility to that of mammalian sperm, it is obvious that parasite male gametes do not rely on oxidative phosphorylation because the male gametes do not possess mitochondria (*24*). This indicates that the driving force for male motility is exclusively supplied from glycolysis. The *in vitro* fertilization assay showed that Pbsdha(-) parasites were defect in ookinete formation. At this moment, it is not clear whether complex II is critical at female gametogenesis, fertilization or ookinete formation itself. Nevertheless, we speculate that the impact of *Pbsdha* gene disruption gave adverse influence on female, probably the stages after gametocytogenesis.

The most drastic phenotypic change in Pbsdha(-) parasites was the complete failure of oocyst formation. In malaria parasites, the ookinetes traverse midgut cell and arrive to the basal lamina where they transform into oocysts. In a single oocyst, mitosis occurs and several hundreds of sporozoites are generated inside. To accomplish such task, the parasites may need more ATP, which could be generated by oxidative phosphorylation. The complex II activity deletion may therefore adversely affect the oocyst formation. Recently, it was reported that NDH2(-) parasites developed normally in asexual stages but transformed into aberrant immature oocysts (*27*). Our present study together with this finding suggests that the ETC enzymes are essential in insect stages. However, there are several phenotypic differences between Pbsdha(-) and NDH2(-) parasites; 1) Pbsdha(-) parasites differentiated into ookinetes with low efficiency, while NDH2(-) ookinete formation is similar to WT parasites. This indicates that the Pbsdha deletion affects an earlier parasite stage compared with that of NDH2 deletion; 2) Pbsdha(-) parasites failed completely in oocyst formation, while NDH2(-) parasites formed immature oocysts with smaller size, demonstrating that the absence of complex II gives more severe defects in parasite development than NDH2 does. In other eukaryotes, it is known that mitochondrial complex II converts succinate to fumarate and reducing equivalents are transferred to quinone. In addition, complex II is one of the TCA cycle members

generating NADH, which is a substrate of NDH2. Thus, the deletion of complex II activity may render NDH2 unable to function in ETC. Severe phenotypic changes in Pbsdha(-) parasites could be therefore attributed to the aberration of NDH2 as well as complex II itself.

Conclusion

In the present work, we show that complex II has a critical role in insect-stage parasites. ETC is not only involved in ATP metabolism, but as well in heme biosynthesis (Fig. 7), which is also crucial for parasite survival (*29*). In addition to the ETC, complex II functions as the TCA cycle enzyme. Further studies are required to determine whether lack of any of these functions are the cause for the developmental arrest in Pbsdha(-) parasites. In any case, our study demonstrates that malaria parasite drastically switches energy metabolism when the parasites initiate sexual maturation and is subsequently introduced into the mosquito (Fig. 7).

The importance of complex II in insect-stage parasites suggests the possibility that complex II could be a novel target for transmission blocking (*30*). Previously, we reported that the amino acid sequences of the membrane anchor subunits CybL and CybS of *Plasmodium* complex II show exceptionally low homology to that of any other organism including human (*12*). In addition, our previous work revealed that atopenin A5 is a potent inhibitor against mammalian complex II with IC_{50} values of three-order of magnitudes lower than that of *Plasmodium* complex II (*13*). This indicates that 3D structure of ubiquinone-binding site in the parasitic complex II is quite distinct from those of mammalian complex II. Therefore, it is conceivable that the development of a parasitic complex II-specific inhibitor would be feasible by structure-based drug design targeting to the mosquito-stages parasite. Currently, further ATP metabolic gene knockout experiment using mouse malaria models are now in progress to draw general view of parasite energy metabolism in response to various environmental stimuli that may have been overlooked in *in vitro* culture systems as pointed out by Daily (*31*).

Acknowledgements

We thank Dr. Terenius for his comments on our manuscript.

Funding

Grants-in-aid for Creative Scientific Research (18GS0314 to KKand YW) and for Scientific Research (C) (21590467 to YY and 20590426 to MH) from the Japanese Society for the Promotion of Science, Targeted Proteins Research Program (to KK) and a Grant-in-aid for Scientific Research on Priority Areas (18073004 to KK and 210220044 to MH) and Grant-in-Aid for Scientific Research on Innovative Areas (22112519 to MH) from the Japanese Ministry of Education, Science, Culture, Sports and Technology, and a grant for research to promote the development of anti-AIDS pharmaceuticals from the Japan Health Sciences Foundation (to KK). This work was also partially suppored by Support Program for Scientific Research Platform in Private Universities (to HM) and SUMITOMO foundation (to MH).

Conflict of interest

None declared.

References

1. Snow, R.W., Guerra, C.A., Noor, A.M., Myint, H.Y., and Hay, S.I. (2005) The global distribution of clinical episodes of *Plasmodium falciparum* malaria. *Nature* **434**, 214–217
2. Petersen, I., Eastman, R., and Lanzer, M. (2011) Drug-resistant malaria: molecular mechanisms and implications for public health. *FEBS Lett.* **585**, 1551–1562
3. Foth, B.J., Stimmler, L.M., Handman, E., Crabb, B.S., Hodder, A.N., and McFadden, G.I. (2005) The malaria parasite *Plasmodium falciparum* has only one pyruvate dehydrogenase complex, which is located in the apicoplast. *Mol. Microbiol.* **55**, 39–53
4. Aikawa, M. (1966) The fine structure of the erythrocytic stages of three avian malarial parasites. *Plasmodium fallax, P. lophurae, and P. cathemerium. Am. J. Trop. Med. Hyg* **15**, 449–471
5. Bryant, C., Voller, A., and Smith, M.J. (1964) The incorporation of radioactivity from (14C)glucose into the soluble metabolic intermediates of malaria parasites. *Am. J. Trop. Med. Hyg* **13**, 515–519
6. Scheibel, L.W. and Pflaum, W.K. (1970) Cytochrome oxidase activity in platelet-free preparations of *Plasmodium falciparum. J. Parasitol.* **56**, 1054
7. Olszewski, K.L., Mather, M.W., Morrisey, J.M., Garcia, B.A., Vaidya, A.B., Rabinowitz, J.D., and Llinas, M. (2010) Branched tricarboxylic acid metabolism in *Plasmodium falciparum. Nature* **466**, 774–778
8. Hall, N., Karras, M., Raine, J.D., Carlton, J.M., Kooij, T.W., Berriman, M., Florens, L., Janssen, C.S., Pain, A., Christophides, G.K., James, K., Rutherford, K., Harris, B., Harris, D., Churcher, C., Quail, M.A., Ormond, D., Doggett, J., Trueman, H.E., Mendoza, J., Bidwell, S.L., Rajandream, M.A., Carucci, D.J., Yates, J.R. 3rd, Kafatos, F.C., Janse, C.J., Barrell, B., Turner, C.M., Waters, A.P., and Sinden, R.E. (2005) A comprehensive survey of the *Plasmodium* life cycle by genomic, transcriptomic, and proteomic analyses. *Science* **307**, 82–86
9. Krungkrai, J., Prapunwattana, P., and Krungkrai, S.R. (2000) Ultrastructure and function of mitochondria in gametocytic stage of *Plasmodium falciparum. Parasite* 7, 19–26
10. Maklashina, E. and Cecchini, G. (2010) The quinone-binding and catalytic site of complex II. *Biochim. Biophys. Acta.* **1797**, 1877–1882
11. Takeo, S., Kokaze, A., Ng, C.S., Mizuchi, D., Watanabe, J.I., Tanabe, K., Kojima, S., and Kita, K. (2000) Succinate dehydrogenase in *Plasmodium falciparum* mitochondria: molecular characterization of the SDHA and SDHB genes for the catalytic subunits, the flavoprotein (Fp) and iron-sulfur (Ip) subunits. *Mol. Biochem. Parasitol.* **107**, 191–205
12. Mogi, T. and Kita, K. (2009) Identification of mitochondrial Complex II subunits SDH3 and SDH4 and ATP synthase subunits a and b in Plasmodium spp. *Mitochondrion* **9**, 443–453
13. Kawahara, K., Mogi, T., Tanaka, T.Q., Hata, M., Miyoshi, H., and Kita, K. (2009) Mitochondrial dehydrogenases in the aerobic respiratory chain of the rodent malaria parasite *Plasmodium yoelii yoelii. J. Biochem.* **145**, 229–237
14. Takashima, E., Takamiya, S., Takeo, S., Mi-ichi, F., Amino, H., and Kita, K. (2001) Isolation of

mitochondria from *Plasmodium falciparum* showing dihydroorotate dependent respiration. *Parasitol. Int.* **50**, 273–278
15. Mather, M.W., Morrisey, J.M., and Vaidya, A.B. (2010) Hemozoin-free *Plasmodium falciparum* mitochondria for physiological and drug susceptibility studies. *Mol. Biochem. Parasitol.* **174**, 150–153
16. Hirai, M., Wang, J., Yoshida, S., Ishii, A., and Matsuoka, H. (2001) Characterization and identification of exflagellation-inducing factor in the salivary gland of *Anopheles stephensi* (Diptera: Culicidae). *Biochem. Biophys. Res. Commun.* **287**, 859–864
17. Dessens, J.T., Beetsma, A.L., Dimopoulos, G., Wengelnik, K., Crisanti, A., Kafatos, F.C., and Sinden, R.E. (1999) CTRP is essential for mosquito infection by malaria ookinetes. *EMBO J.* **18**, 6221–6227
18. Janse, C.J., Ramesar, J., and Waters, A.P. (2006) High-efficiency transfection and drug selection of genetically transformed blood stages of the rodent malaria parasite *Plasmodium berghei*. *Nat. Protoc.* **1**, 346–356
19. Jensen, J.B. and Trager, W. (1977) *Plasmodium falciparum* in culture: use of outdated erthrocytes and description of the candle jar method. *J. Parasitol.* **63**, 883–886
20. Kobayashi, T., Sato, S., Takamiya, S., Komaki-Yasuda, K., Yano, K., Hirata, A., Onitsuka, I., Hata, M., Miichi, F., Tanaka, T., Hase, T., Miyajima, A., Kawazu, S., Watanabe, Y., and Kita, K. (2007) Mitochondria and apicoplast of *Plasmodium falciparum*: behaviour on subcellular fractionation and the implication. *Mitochondrion* **7**, 125–132
21. Chan, M., Tan, D.S., Wong, S.H., and Sim, T.S. (2006) A relevant in vitro eukaryotic live-cell system for the evaluation of plasmodial protein localization. *Biochimie* **88**, 1367–1375
22. van Dijk, M.R., Janse, C.J., Thompson, J., Waters, A.P., Braks, J.A., Dodemont, H.J., Stunnenberg, H.G., van Gemert, G.J., Sauerwein, R.W., and Eling, W. (2001) A central role for P48/45 in malaria parasite male gamete fertility. *Cell* **104**, 153–164
23. Okamoto, N., Spurck, T.P., Goodman, C.D., and McFadden, G.I. (2009) Apicoplast and mitochondrion in gametocytogenesis of *Plasmodium falciparum*. *Eukaryot. Cell* **8**, 128–132
24. Mogi, T. and Kita, K. (2010) Diversity in mitochondrial metabolic pathways in parasitic protists *Plasmodium* and *Cryptosporidium*. *Parasitol. Int.* **59**, 305–312
25. van Dooren, G.G., Marti, M., Tonkin, C.J., Stimmler, L.M., Cowman, A.F., and McFadden, G.I. (2005) Development of the endoplasmic reticulum, mitochondrion and apicoplast during the asexual life cycle of *Plasmodium falciparum*. *Mol. Microbiol.* **57**, 405–419
26. Daily, J.P., Scanfeld, D., Pochet, N., Le Roch, K., Plouffe, D., Kamal, M., Sarr, O., Mboup, S., Ndir, O., Wypij, D., Levasseur, K., Thomas, E., Tamayo, P., Dong, C., Zhou, Y., Lander, E.S., Ndiaye, D., Wirth, D., Winzeler, E.A., Mesirov, J.P., and Regev, A. (2007) Distinct physiological states of *Plasmodium falciparum* in malaria-infected patients. *Nature* **450**, 1091–1095
27. Boysen, K.E. and Matuschewski, K. (2011) Arrested oocyst maturation in *Plasmodium* parasites lacking type II NADH:ubiquinone dehydrogenase. *J. Biol. Chem.* **286**, 32661–3271
28. Nascimento, J.M., Shi, L.Z., Tam, J., Chandsawangbhuwana, C., Durrant, B., Botvinick, E.L., and Berns, M.W. (2008) Comparison of glycolysis and oxidative phosphorylation as energy sources for mammalian sperm motility, using the combination of fluorescence imaging, laser tweezers, and real-time automated tracking and trapping. *J. Cell Physiol.* **217**, 745–751
29. Nagaraj, V.A., Arumugam, R., Prasad, D., Rangarajan, P.N., and Padmanaban, G. (2010) Protoporphyrinogen IX oxidase from *Plasmodium falciparum* is anaerobic and is localized to the mitochondrion. *Mol. Biochem. Parasitol.* **174**, 44–52
30. Lavazec, C. and Bourgouin, C. (2008) Mosquito-based transmission blocking vaccines for interrupting *Plasmodium* development. *Microbes Infect.* **10**, 845–849
31. LeRoux, M., Lakshmanan, V., and Daily, J.P. (2009) *Plasmodium falciparum* biology: analysis of in vitro versus in vivo growth conditions. *Trends Parasitol.* **25**, 474–481

Parasitology International 61 (2012) 726–728

Contents lists available at SciVerse ScienceDirect

Parasitology International

journal homepage: www.elsevier.com/locate/parint

Short communication

Toward understanding the role of mitochondrial complex II in the intraerythrocytic stages of *Plasmodium falciparum*: Gene targeting of the Fp subunit

Takeshi Q. Tanaka [a,1], Makoto Hirai [b], Yoh-ichi Watanabe [a,*], Kiyoshi Kita [a,*]

[a] Department of Biomedical Chemistry, Graduate School of Medicine, The University of Tokyo, 7-3-1 Hongo, Bunkyo-ku, Tokyo 113-0033, Japan
[b] Department of Parasitology, Graduate School of Medicine, Gunma University, 3-39-22 Maebashi City, Gunma 371-8511, Japan

ARTICLE INFO

Article history:
Received 3 April 2012
Received in revised form 1 June 2012
Accepted 5 June 2012
Available online 12 June 2012

Keywords:
Malaria
Intraerythrocytic stage
Tricarboxylic acid cycle
Succinate

ABSTRACT

Malaria parasites in human hosts depend on glycolysis for most of their energy production, and the mitochondrion of the intraerythrocytic form is acristate. Although the genes for all tricarboxylic acid (TCA) cycle members are found in the parasite genome, the presence of a functional TCA cycle in the intraerythrocytic stage is still controversial. To elucidate the physiological role of *Plasmodium falciparum* mitochondrial complex II (succinate-ubiquinone reductase (SQR) or succinate dehydrogenase (SDH)) in the TCA cycle, the gene for the flavoprotein subunit (Fp) of the enzyme, *pfsdha* (*P. falciparum* gene for SDH subunit A, PlasmoDB ID: PF3D7_1034400) was disrupted. SDH is a well-known marker enzyme for mitochondria. In the *pfsdha* disruptants, Fp mRNA and polypeptides were decreased, and neither SQR nor SDH activity of complex II was detected. The suppression of complex II caused growth retardation of the intraerythrocytic forms, suggesting that complex II contributes to intraerythrocytic parasite growth, although it is not essential for survival. The growth retardation in the *pfsdha* disruptant was rescued by the addition of succinate, but not by fumarate. This indicates that complex II functions as a quinol-fumarate reductase (QFR) to form succinate from fumarate in the intraerythrocytic parasite.

Many aerobic organisms, including humans, depend on oxidative phosphorylation for most of their energy metabolism. On the other hand, the intraerythrocytic malaria parasite synthesizes ATP by anaerobic glycolysis [1]. All the genes for the glycolytic pathway are found in the parasite genome, and pyruvate generated from glucose by glycolysis is converted to lactate with NAD^+ generation [2,3]. The role of mitochondria in parasite energy metabolism is unclear. β-oxidation is absent from the mitochondria and there is no biochemical evidence for a canonical and functional tricarboxylic acid (TCA) cycle in the intraerythrocytic form [2,4,5].

In mammals, mitochondrial complex II functions as a succinate-ubiquinone reductase (SQR) that catalyzes the oxidation of succinate in the TCA cycle and supplies electrons to the respiratory chain. Generally, complex II is composed of four subunits: a flavoprotein subunit (Fp) and an iron–sulfur protein subunit (Ip) as catalytic domains, and two hydrophobic subunits as membrane anchor domains. The genes for the Fp and Ip, *pfsdha* (PlasmoDB ID: PF3D7_1034400) and *pfsdhb*, have been cloned, and *P. falciparum* mitochondrial proteins show both succinate dehydrogenase (SDH) and SQR activities, indicating that complex II should have some role in parasite survival [6,7]. On the other hand, complex II functions as a quinol-fumarate reductase (QFR), the reverse action of SQR, for anaerobic respiration in various anaerobic organisms [8]. Thus, the direction of the reaction suggests the biological function of complex II.

Since mitochondrial complex II was potentially expected to be essential for parasite survival, a tetracycline analogue-regulated transgene expression system in *P. falciparum* was chosen to establish a conditional knockout strain for the analysis of this potentially essential gene [9]. Since this is a Tet-Off system, the target gene under control is expressed in the absence of the tetracycline analogue anhydrotetracycline (ATc), and the addition of ATc should repress the target gene expression. A conditional knockout of the gene for the Fp subunit in SQR from *P. falciparum* was tried with a pTGPI-GFP derived vector, by which the target gene expression could be controlled with ATc in the parasite (Fig. 1) [9].

As pTGPI-GFP is a 'Tet-Off' system, the transformants were cultured in a medium without ATc, to keep *pfsdha* expression. Stable recombinant parasites had been cloned by limiting dilution from pTSDHA-trunc and pTSDHA-full transformants. The genomic organization of the targeted loci was confirmed by Southern blotting (not shown).

To analyze the *pfsdha* transcription, total RNAs from the trophozoite/schizont-rich culture were used for semi-quantitative RT-PCR and Northern blot analysis. Unexpectedly, the *pfsdha* disruptant did not express *pfsdha* mRNA even in the absence of ATc (not shown). These results indicate that the established *pfsdha* disruptants were not conditional

* Corresponding authors. Tel.: +81 3 5841 3528; fax: +81 3 5841 3444.
E-mail addresses: ywatanab@m.u-tokyo.ac.jp (Y. Watanabe), kitak@m.u-tokyo.ac.jp (K. Kita).
[1] Present address: Laboratory of Malaria and Vector Research, National Institute of Allergy and Infectious Diseases, National Institutes of Health, Rockville, MD 20892, United States.

1383-5769/$ – see front matter © 2012 Elsevier Ireland Ltd. All rights reserved.
doi:10.1016/j.parint.2012.06.002

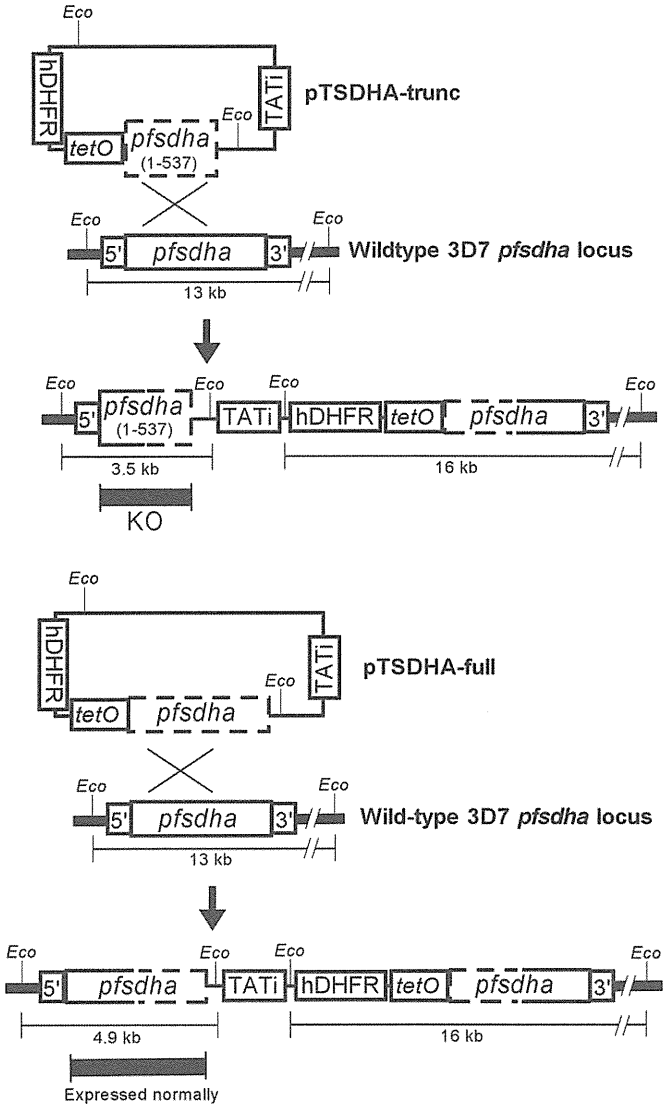

Fig. 1. (A) Schematic diagrams for '*pfsdha* disruption' and the control integration into the target locus. The *pfsdha* gene (1–537 and full-length), human dihydrofolate reductase (hDHFR), tetracycline repressor and transactivator fusion protein (TATi3), tetracycline operator sequence (*tetO*), and the *Eco*RV site (*Eco*) are labeled. Thin and thick solid lines indicate the backbone sequences of the plasmid and the 3D7 chromosomal DNA, respectively. Parasites were cultured following standard protocols [17]. *P. falciparum* (3D7 strain) were cultivated according to [10] with slight modifications. The parental plasmid, pTGPI-GFP, was a kind gift from Dr. B.S. Crabb (Walter and Eliza Hall Institute of Medical Research, Australia) [9]. Since the Rep20 element in pTGPI-GFP is a subtelomeric repeated region and localizes the plasmid to perinuclear chromosome-end clusters [18], and it was expected to potentially inhibit plasmid integration into the homologous chromosomal locus, pTGPI-GFPΔRep20 plasmid was obtained from pTGPI-GFP with *Bgl*II digestion and self-ligation. A DNA fragment of *pfsdha* (GenBank ID: XM_001347582, PlasmoDB ID: PF3D7_1034400) corresponding to nucleotide coding region 1–537 with additional sequences of *Sse*8387I and *Spe*I sites at each end, allowing for insertion between the *Pst*I and *Spe*I sites of pTGPI-GFP, was amplified by PCR from 3D7 genomic DNA prepared with DNAzol (Invitrogen, Life Technologies). The PCR product was digested with *Sse*8387I and *Spe*I and then inserted into the digested pTGPI-GFPΔRep20, resulting in plasmid pTSDHA-trunc. As a control, a DNA fragment of full-length *pfsdha* with additional sequences of *Sse*8387I and *Spe*I sites at each end was amplified by PCR from genomic DNA. The fragment was cloned between the *Pst*I and *Spe*I sites of pTGPI-GFPΔRep20 by the same method as above, resulting in plasmid pTSDHA-full. The primer sequences were available from the authors upon request. Plasmid DNA was electroporated to infected erythrocytes and transfected parasites were selected with 5 nM WR99210 (Jacobus Pharmaceutical Co., Inc., Princeton, NJ, USA, a kind gift of Dr. David Jacobs) [19]. Single-cell cloning was carried out by limiting dilution.

knockouts, but constitutively *pfsdha*-repressed strains. In a previous study, a similar phenomenon was observed in parasites cultured for prolonged periods (Dr. B.S. Crabb, personal communication). These mutants were useful for the study on the role of complex II in intraerythrocytic form as constitutively *pfsdha*-repressed mutants although the *pfsdha* disruptants were not expected mutants.

Following the analysis of the transcription of *pfsdha* gene, the expression of Fp and Ip peptides was examined by Western blot analysis with mitochondrial proteins prepared from trophozoite/schizont-rich culture [10]. The expression of Fp protein in the mitochondrial fraction from the *pfsdha* disruptant was significantly lower than that of the other controls (not shown). Interestingly, in spite of the normal expression of the *pfsdhb* transcript, repression of Ip protein was observed in the *pfsdha* disruptant (not shown). Although their expressions were not completely repressed, both of the signal intensities for the Fp and Ip proteins of the *pfsdha* disruptant should be low enough to evaluate its role.

The enzyme activities of complex II and dihydroorotate dehydrogenase (DHOD) were examined with mitochondrial proteins isolated from the parasites according to [10]. DHOD is the fourth enzyme of the *de novo* pyrimidine synthetic pathway. *P. falciparum* DHOD localizes on the mitochondrial membrane and transfers electrons to ubiquinone in the respiratory chain [11]. Both SDH and SQR activities in mitochondria from the *pfsdha* disruptant, examined according to [7,10], were repressed to undetectable levels, while mitochondria from the controls showed 3.84 to 6.15 nmol/min/mg of SDH and 3.11 to 5.45 nmol/min/mg of SQR activities. On the other hand, there was no difference in DHOD activities between the controls (13.9 to 18.9 nmol/min/mg) and the *pfsdha* disruptant (15.7 nmol/min/mg).

To examine the effect of Fp repression, parasite growth was analyzed after a 48-h culture, one intraerythrocytic growth cycle. As shown in Fig. 2A, the growth retardation was detected in experiments started at 0.2% parasitemia (gray bars). The parasitemia of the controls was $1.78 \pm 0.14\%$ (wild type), $1.73 \pm 0.15\%$ (control of plasmid transfection), and $1.70 \pm 0.15\%$ (control of integration). Meanwhile, the parasitemia of the *pfsdha* disruptant was $0.94\% \pm 0.09\%$, half of that for the controls (Fig. 2A).

Succinate and fumarate are substrates for SQR and QFR, respectively. The direction of the complex II reaction was examined by the addition of the substrates to the *pfsdha* disruptant. The maximum concentration of succinate and fumarate used was 5 mM, because the intraerythrocytic parasite cannot survive in a culture medium with $\geq$50 mM succinate or fumarate (not shown). As a result, 5 mM of succinate rescued the growth retardation of the *pfsdha* disruptant, but fumarate did not (Fig. 2B). The growth of the controls was not affected by the substrate addition. To examine the dose response, the parasites were incubated with between 5 mM and 50 nM of succinate or fumarate. Growth retardation rescue was observed in the *pfsdha* disruptant with $\geq$50 μM of succinate, but fumarate did not rescue the parasite growth retardation (Fig. 2B). These findings suggest that complex II catalyzes succinate production by fumarate reduction in the intraerythrocytic forms.

If the volume of cell and protein concentration [12] is taken account, the concentrations of succinate and fumarate in human cell [13] could be equivalent to those in the parasite (10^{-1} mM) [14]. Thus, under physiological condition, growth retardation of the disruptant in the intraerythrocytic stages may not be observed.

Complex II appears to function as a QFR, and the produced succinate is required in other metabolic pathways. Heme biosynthesis might be a potential pathway that needs the produced succinate, because succinate could be a precursor of succinyl-CoA for the first step of heme biosynthesis. Moreover, QFR has been proposed to couple with protoporphyrinogen IX oxidase in the heme biosynthesis pathway of *P. falciparum* [15]. Our previous observation showing functional link between dihydroorotate-dependent respiration and QRF [7] is consistent with this idea. Considering that a recent report suggested branched TCA cycle metabolism in the parasite [16], further biochemical analysis is indispensable to understand the real nature of the energy metabolism of the parasite.

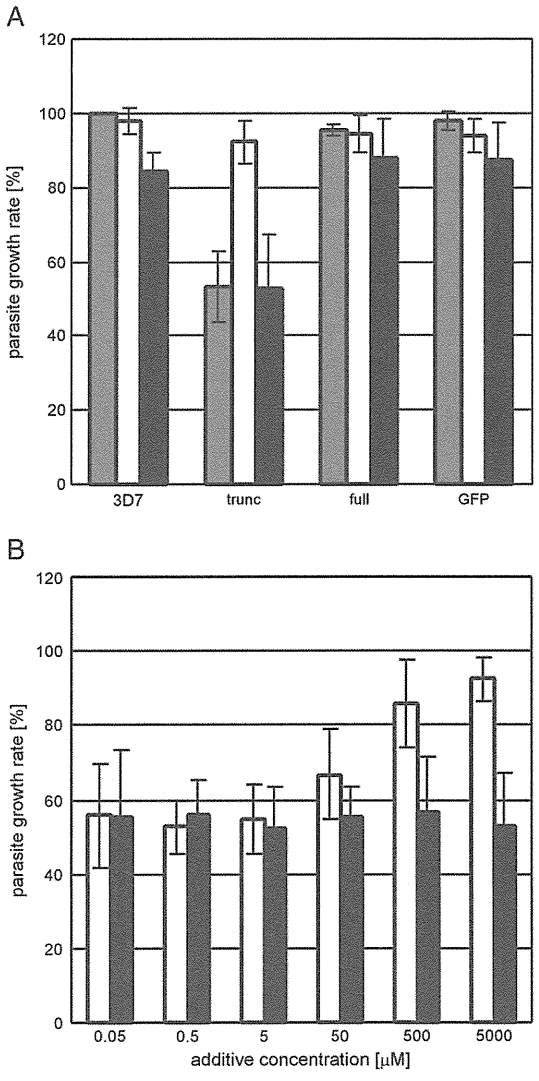

Fig. 2. (A) Growth retardation of the *pfsdha* disruptant and growth rescue by substrates. Gray, white, and black bars indicate no additives, 5 mM of succinate, and 5 mM of fumarate, respectively. (B) Dose dependency of succinate on growth rescue in the *pfsdha* disruptant (pTSDHA-trunc clonal line). White and black bars indicate succinate (Suc) and fumarate (Fum) addition to the *pfsdha* disruptant, respectively. 3D7, wild-type 3D7 strain; trunc, pTSDHA-trunc clonal line ('*pfsdha* disruptant'); full, pTSDHA-full clonal line; GFP, pTGPI-GFPΔRep20 transformant. Synchronized parasites, prepared according to [20], at 0.2% starting parasitemia were triplicated with 1 ml each of complete medium containing 0.5% (w/v) AlbuMAX I (Gibco, Life Technologies). Giemsa-stained smears were prepared after a 48-h incubation without media change, and the parasitemia was evaluated by optical microscopy.

Acknowledgment

This work was supported in part by Grants-in-aid for Creative Scientific Research (18GS0314 to KK and YW) and for Scientific Research (C) (21590467 to YW) from the Japanese Society for the Promotion of Science, Targeted Proteins Research Program (to KK), a Grant-in-aid for Scientific Research on Priority Areas (18073004 to KK) from the Japanese Ministry of Education, Science, Culture, Sports and Technology, and a grant for research to promote the development of anti-AIDS pharmaceuticals from the Japan Health Sciences Foundation (to KK).

We thank Dr. B.S. Crabb and the Walter and Eliza Hall Institute of Medical Research for their kind gift of the pTGPI-GFP vector, and Jacobus Pharmaceuticals for its gift of WR99210. We also thank Prof. K. Tanabe (Osaka University) for his critical advice about the growth experiment of the parasite, Ms. A. Hino (University of Tokyo) for the help in the manuscript preparation, and Dr. Emmanuel O. Balogun (University of Tokyo) for the language correction.

References

[1] Roth Jr E. *Plasmodium falciparum* carbohydrated metabolism: a connection between host cell and parasite. Blood Cells 1990;16:453–60.
[2] Gardner MJ, Hall N, Fung E, White O, Berriman M, Hyman RW, et al. Genome sequence of the human malaria parasite *Plasmodium falciparum*. Nature 2002;419:498–511.
[3] Makler MT, Hinrichs DJ. Measurement of the lactate dehydrogenase activity *Plasmodium falciparum* as an assessment of parasitemia. The American Journal of Tropical Medicine and Hygiene 1993;48:205–10.
[4] Blum JJ, Ginsburg H. Absence of alpha-ketoglutarate dehydrogenase activity and presence of CO_2-fixing activity in *Plasmodium falciparum* grown in vitro in human erythrocytes. The Journal of Protozoology 1984;31:167–9.
[5] Lang-Unnasch N. Purification and properties of *Plasmodium falciparum* malate dehydrogenase. Molecular and Biochemical Parasitology 1992;50:17–25.
[6] Takeo S, Kokaze A, Ng CS, Mizuchi D, Watanabe J, Tanabe K, et al. Succinate dehydrogenase in *Plasmodium falciparum* mitochondria: molecular characterization of the SDHA and SDHB genes for the catalytic subunits, the flavoprotein (Fp) and iron–sulfur (Ip) subunits. Molecular and Biochemical Parasitology 2000;107:191–205.
[7] Takashima E, Takamiya S, Takeo S, Mi-ichi F, Amino H, Kita K. Isolation of mitochondria from *Plasmodium falciparum* showing dihydroorotate dependent respiration. Parasitology International 2001;50:273–8.
[8] Sakai C, Tomitsuka E, Esumi H, Harada S, Kita K. Mitochondrial fumarate reductase as a target of chemotherapy: from parasites to cancer cells. Biochimica et Biophysica Acta 2012;1820:643–51.
[9] Meissner M, Krejany E, Gilson PR, de Koning-Ward TF, Soldati D, Crabb BS. Tetracycline analogue-regulated transgene expression in *Plasmodium falciparum* blood stages using *Toxoplasma gondii* transactivators. Proceedings of the National Academy of Sciences of the United States of America 2005;102:2980–5.
[10] Kobayashi T, Sato S, Takamiya S, Komaki-Yasuda K, Yano K, Hirata A, et al. Mitochondria and apicoplast of *Plasmodium falciparum*: behaviour on subcellular fractionation and the implication. Mitochondrion 2007;7:125–32.
[11] Krungkrai J. Purification, characterization and localization of mitochondrial dihydroorotate dehydrogenase in *Plasmodium falciparum*, human malaria parasite. Biochimica et Biophysica Acta 1995;1243:351–60.
[12] Valverde D, Quintero MR, Candiota AP, Badiella L, Cabañas ME, Arús C. Analysis of the changes in the ^{1}H NMR spectral pattern of perchloric acid extracts of C6 cells with growth. NMR in Biomedicine 2006;19:223–30.
[13] Pollard PJ, Brière JJ, Alam NA, Barwell J, Barclay E, Wortham NC, et al. Accumulation of Krebs cycle intermediates and over-expression of HIF1α in tumours which result from germline FH and SDH mutations. Human Molecular Genetics 2005;14:2231–9.
[14] Teng R, Junankar PR, Bubb WA, Rae C, Mercier P, Kirk K. Metabolite profiling of the intraerythrocytic malaria parasite *Plasmodium falciparum* by ^{1}H NMR spectroscopy. NMR in Biomedicine 2009;22:292–302.
[15] Nagaraj VA, Arumugam R, Prasad D, Rangarajan PN, Padmanaban G. Protoporphyrinogen IX oxidase from *Plasmodium falciparum* is anaerobic and is localized to the mitochondrion. Molecular and Biochemical Parasitology 2010;174:44–52.
[16] Olszewski KL, Mather MW, Morrisey JM, Garcia BA, Vaidya AB, Rabinowitz JD, et al. Branched tricarboxylic acid metabolism in *Plasmodium falciparum*. Nature 2010;466:774–8.
Erratum in:Nature 2010;469:432.
[17] Trager W, Jensen JB. Human malaria parasites in continuous culture. Science 2004;193:673–5.
[18] O'Donnell RA, Freitas-Junior LH, Preiser PR, Williamson DH, Duraisingh M, McElwain TF, et al. A genetic screen for improved plasmid segregation reveals a role for Rep20 in the interaction of *Plasmodium falciparum* chromosomes. The EMBO Journal 2002;21:1231–9.
[19] Wu Y, Sifri CD, Lei HH, Su XZ, Wellems TE. Transfection of *Plasmodium falciparum* within human red blood cells. Proceedings of the National Academy of Sciences of the United States of America 1995;92:973–7.
[20] Lambros C, Vanderberg JP. Synchronization of *Plasmodium falciparum* erythrocytic stages in culture. The Journal of Parasitology 1979;65:418–20.